ADAPTIVE BEAMFORMING FOR OFDM SYSTEMS

By

NC SAMRA JABEEN (SYN LDR)
NC SHAHEER NAEEM
NC ALI IMAM
NC SANA AJMAL

PROJECT DS: LT COL (R) JAVED HUSSAIN BANGASH (INTERNAL)
LT COL DR. SHOAIB AHMED KHAN (EXTERNAL)

A thesis submitted to the faculty of Electrical Engineering Department, Military College of Signals, National University of Sciences and Technology, Rawalpindi in partial fulfillment of the requirements of MCS/NUST for the award of B.E degree in Telecommunication engineering.

APRIL 2007

Dedicated To Our Parents, Without Whose Love and Support We Could Not Have Achieved This

ACKNOWLEDGEMENTS

We thank Almighty Allah for granting us success in completing this project. We would also like to thank our families, who never stopped encouraging us to work hard and kept our hopes high.

The Faculty of Electrical Engineering has been a great help and has constantly provided us with whatever help we needed. Lt Col (R) Javed Hussain Bangash has been a great help in every way possible and we would like to thank him for his immense help and efforts and for his role as our advisor and mentor. Lt Col Shoaib Ahmed Khan(CASE) has dedicated time and efforts to guide us, making valuable contributions.

We would also like to express our deepest gratitude to all the authors, researchers, engineers and analysts whose work has enabled us to accomplish this task, a special note of thanks to all those who helped us personally with their expertise.

We could be forgetting some vital contributors but we appreciate and regard the efforts of everybody who lend a helping hand to us in the project.

ABSTRACT

Adaptive antennas provide an efficient means for minimizing channel interferences by directing the antenna beam towards the desired signal/transmitter and placing a null towards the interfering signal. Orthogonal Frequency Division Multiplexing (OFDM) is gaining popularity for high data rate communication systems. OFDM is different from the conventional multicarrier techniques as it sends information on a number of overlapping orthogonal subcarriers by dividing the total signal bandwidth. To modulate the signal on these subcarriers Inverse Fast Fourier Transform (IFFT) is used on the transmitter. OFDM is less susceptible to Inter Symbol Interference introduced in the multipath environment because its symbol duration is long compared with the data symbols in the serial data stream. In order to completely eliminate ISI a cyclic guard time longer than the channel delay is prepended to every OFDM symbol maintaining the orthogonality among subcarriers. However, the symbols still experience interference from their replicas originating from multipaths. This is termed as self-interference. Under the assumptions of narrowband model a phase shift is introduced in each multipath component. One solution for removal of this phase shift is equalization, requiring channel estimation which is not possible when the power of the interfering signal is higher than the desired signal. The approach we suggest bypasses equalization and employs an antenna array with an adaptive beamforming algorithm for interference rejection in OFDM systems. The Fast Fourier Transform (FFT) is employed at the receiver end of an OFDM system to demodulate the baseband symbol, which enables the use of frequency domain beamforming. In frequency domain beamforming, a separate beamformer for each subcarrier, having its own set of weight vector can be implemented. In case of frequency selective channel the distortion introduced in each subcarrier of an OFDM symbol is different. Similarly narrow band interference distorts only a portion of signal bandwidth. Thus, a separate beamformer for each subcarrier allows the suppression of these distortions. The weight vectors of the beamformer are iteratively updated using adaptive algorithm. Both the decision directed and blind algorithms are implemented in this project.

DECLARATION

It is hereby declared that this is our own work and has not been submitted in any form for another degree or diploma at any other university or institution for tertiary education. Information derived from published or unpublished work of others has been acknowledged in the text and a list of references is given.

TABLE OF CONTENTS

LIST OF FIGURES

Number *Page*

MOTIVATION

Wireless communication has come a long way. In recent years there has been an explosive growth in the number of wireless users particularly in the area of mobile communication. The wireless mobile systems are becoming increasingly sophisticated and widespread. This growth has triggered an enormous demand for greater capacity, better coverage and higher quality of service and the future 4G mobile systems aim at the same [1].

To support high data rates, wideband carriers are required. The problem with such carriers is that they suffer distortion in a channel due to frequency selective fading in a multipath environment. This motivates the use of Orthogonal Frequency Division Multiplexing (OFDM) since it is less susceptible to inter-symbol interference (ISI) introduced in the multipath environment [2]. However, OFDM systems are vulnerable to inter-channel interference (ICI). If inter-channel interferences are strong and bursty, conventional OFDM receivers are not able to cancel them. An adaptive antenna array deployed at the receiver, combined with OFDM, is able to enhance the signal integrity in an interference environment by suppressing ICI [3]. Antenna arrays can also reject interference caused by jamming signals by acting as a spatial filter which separates the desired signal from the interfering signal. Adaptive beamforming uses antenna arrays backed by strong signal processing capability to automatically change the beam pattern in accordance with the changing signal environment. Due to its advantages, an adaptive antenna array is likely to be an integral part of the 4G systems.

Internationally, little research work has been done for smart antenna application to OFDM systems and investigating interference suppression capability for multi-path environments. The nature of modulation/demodulation on subcarriers in an OFDM system requires a new approach for implementing adaptive algorithms on the antenna array. Therefore, it is necessary to understand the fundamental principle of OFDM and to develop techniques for applying adaptive array algorithms to OFDM systems.

OBJECTIVE OF THE PROJECT

1. To apply adaptive array algorithms to an OFDM system, investigate its interference suppression capability for multipath environments and for jamming signals.
2. To carry out the performance analysis of various adaptive beamforming algorithms by simulating them on MATLAB and comparing their simulation results.
3. To carry out the hardware implementation of the adaptive algorithms on the DSK TMS32067xx platform.

OUTLINE OF THE THESIS

Chapter 1 introduces the fundamentals of OFDM It covers the basic concept, the process, channel effects and the receiver end.

Chapter 2 introduces the fundamentals of adaptive antenna arrays. It defines different antenna array configurations, discusses the structure and working of Uniform Linear Arrays, and the use of antenna arrays for spatial filtering.

Chapter 3 presents a detailed analysis of adaptive antenna array systems. Different types of adaptive antenna systems are discussed here. Also, their working mechanism is reviewed, along with their classifications. This chapter also addresses the issue of multipath. Then it moves on to the concept of beamforming, covering narrowband, wideband and frequency domain beamformers. At the end it highlights the benefits and applications of adaptive antennas.

Chapter 4 discusses adaptive beamforming applied in the antenna arrays. Criterion for updating the weights is also reviewed. This is followed by an in-depth analysis of different adaptation techniques which use adaptive filters. Then, the adaptive beamforming algorithms used are explained.

Chapter 5 focuses on the adaptive beamforming algorithms used in the project. A detailed analysis of the adaptive beamforming algorithms is given and they are explained along with their simulation results, derived in MATLAB. Finally, detailed comparisons of the BER performance of the different beamforming algorithms in various simulation cases are provided at the end of this chapter.

Chapter 6 The adaptive beamforming algorithm proposed for the OFDM system is described in detail, with all the supporting simulation results in MATLAB. Also, the structure of the frequency-domain beamformer is provided. A study of the proposed beamforming algorithm is presented for a two-ray channel model. In this chapter, the structure of the transmitter and receiver used in the simulation are also described.

Chapter 7 Addresses the implementation of the adaptive beamforming algorithms on the DSP Starters' Kit TMS3206713. It includes installation, architecture and information regarding Code Composer Studio v 3.1

Chapter 8 In this chapter conclusion for the entire project, along with some suggestions is presented. It also provides useful guidelines for any future work in this field.

CHAPTER 1: INTRODUCTION TO OFDM

1.1. Introduction

Wireless system is required to accommodate as many users as possible by effectively sharing the limited bandwidth. In older multi-channel systems using FDM, the total available bandwidth is divided into N *non-overlapping* frequency sub-channels. Each sub-channel is modulated with a separate symbol stream and the N sub-channels are frequency multiplexed. Even though the prevention of spectral overlapping of sub-carriers reduces Inter-channel Interference, this leads to inefficient use of spectrum. The guard bands on either side of each sub-channel are a waste of precious bandwidth. To overcome the problem of bandwidth wastage, we can instead use N overlapping (but orthogonal) subcarriers, each carrying a symbol rate of 1/T and spaced 1/T apart.

1.2. Orthogonality

Orthogonality is a property that allows multiple information signals to be transmitted perfectly over a common channel and detected, without interference. This permits the proper demodulation of the symbol streams without the requirement of non-overlapping spectra. Another way of specifying the subcarrier orthogonality condition is to require that each sub-carrier has exactly integer number of cycles in the interval T.

Orthogonal Frequency Division Multiplexing (OFDM) is a multicarrier modulation scheme, in which the bandwidth of the channel is divided into subcarriers and high-rate data stream is divided into multiple low-rate parallel data streams, which are modulated and transmitted on each subcarrier simultaneously. These subcarriers are overlapping and orthogonal in nature, making OFDM spectrally more efficient and eliminating interference from one subcarrier to another.

This greatly simplifies the design of both the transmitter and the receiver. Unlike conventional Frequency Division Multipleixng (FDM), a separate filter for each subcarrier is not required. Orthogonality also allows high spectral efficiency, near the Nyquist rate. Almost the whole available frequency band can be utilized. OFDM

generally has a nearly 'white' spectrum, giving it benign electromagnetic interference properties with respect to other co-channel users. Orthogonality allows for efficient modulator and demodulator implementation using the Fast Fourier Transform (FFT) algorithm. Although the principles and some of the benefits have been known since long, OFDM is popular for wideband communications today by way of low-cost digital signal processing components that can efficiently calculate the FFT.

Orthogonality can be explained by two ways. Firstly, notice in figure 1.1, that each carrier has an integer number of cycles in the time interval T, and the number of cycles between adjacent subcarriers differs by exactly one. This results in the desired output by integration (through IFFT) for the particular subcarrier, while giving zero result for all other subcarriers. This property accounts for orthogonality between subcarriers.

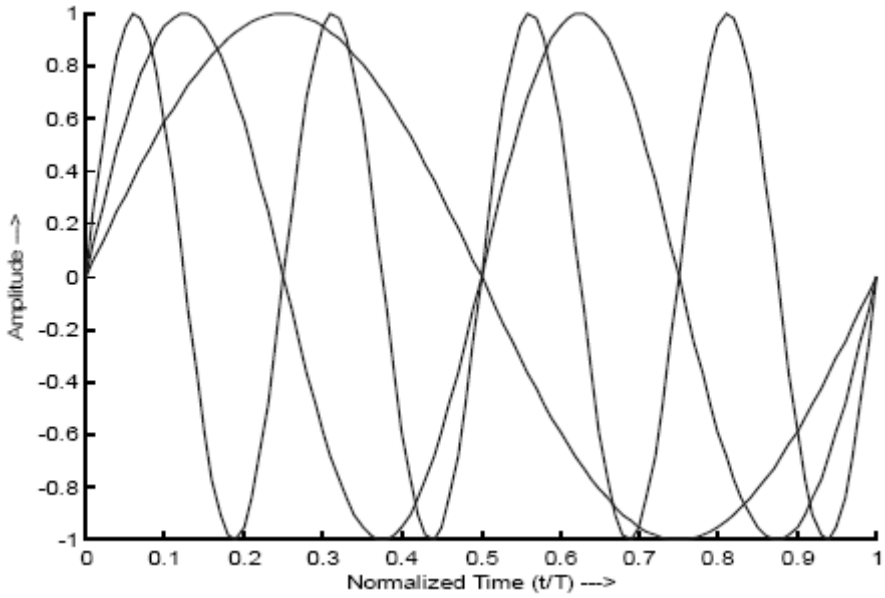

Figure 1.1: Three subcarriers within an OFDM symbols[2]

Another way of viewing the orthogonality property is through frequency domain analysis, as shown in figure 1.2. Each OFDM symbol contains subcarriers that are non-zero over T-second interval. The spectrum of a single symbol is a convolution of a group of pulses located at the subcarrier frequencies, with the spectrum of a square pulse that is one for a T-second period and zero otherwise. At the maximum of each subcarrier spectrum, all

other subcarrier spectra are zero. Because an OFDM receiver essentially calculates the spectrum values at those points that correspond to the maxima of individual subcarriers, it can demodulate each subcarrier free from interference from any other subcarrier, thus avoiding interchannel interference (ICI).

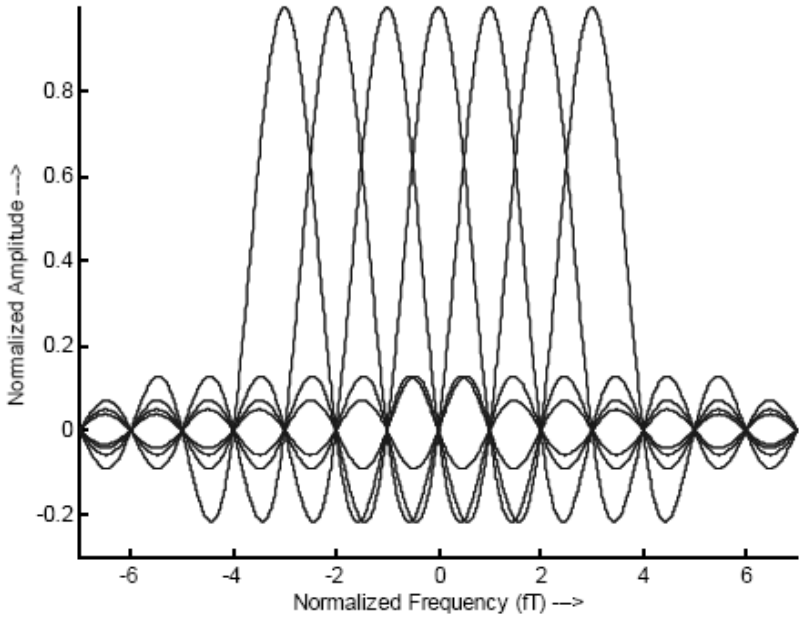

Figure 1.2: Spectra of individual subcarriers[2]

OFDM requires very accurate frequency synchronisation between the receiver and the transmitter; any deviation would destroy the orthogonality of the sub-carriers leading to inter-carrier interference (ICI) or cross-talk between the sub-carriers.

1.3 Generation of OFDM Symbols

A baseband OFDM symbol can be generated in the digital domain before modulating on a carrier for transmission. To generate a baseband OFDM symbol, a serial of digitized data stream is first modulated using common modulation schemes such as the phase shift keying (PSK). These data symbols are then converted from serial-to-parallel (S/P) before modulating subcarriers. Subcarriers are sampled with sampling rate N/Ts, where N is the number of subcarriers and Ts is the OFDM symbol duration. The frequency separation between two adjacent subcarriers is $2\pi/N$. Finally, samples on each subcarrier are summed together to form an OFDM symbol. An OFDM symbol generated by an N-

subcarrier OFDM system consists of *N* samples and the *m*-th sample of an OFDM symbol is [5]

$$x_m = \sum_{k=0}^{N-1} X_k \exp\left\{ j \frac{2\pi mn}{N} \right\}, 0 \le m \le N-1 \qquad (1.1)$$

where *Xn* is the transmitted data symbol on the *n*-th subcarrier. Equation 1.1 is equivalent to the *N*-point inverse discrete Fourier transform (IDFT) operation on the data sequence with the omission of a scaling factor. IDFT can be implemented efficiently using inverse fast Fourier transform (IFFT). Therefore, in practice, the IFFT is performed on the data sequence at an OFDM transmitter for baseband modulation and the FFT is performed at an OFDM receiver for baseband demodulation. Finally, a baseband OFDM symbol is modulated by a carrier and transmitted to the receiver. In the frequency domain, this corresponds to translating all the subcarriers from baseband to the carrier frequency simultaneously. Figure 1.3 shows a 4-subcarrier OFDM transmitter and the process of generating one OFDM symbol.

1.3.1 Symbol Mapping (QPSK)

In order to utilize the bandwidth to maximum efficiency to attain a higher signaling rate, a number of bits are mapped into symbols. Symbols are formed by combination of M bits, each M set of bits representing 2^M symbols. The bandwidth is dependent on signaling rate so by using symbol mapping you can efficiently utilize the bandwidth but the consideration of trade off between receiver complexity in level detection and number of bits should also be taken into account while mapping the bits into symbols; also increasing the number of bits per symbol reduces noise margin.

For quadrature symbol mapping, we divide the input signal array into the matrix with nx4 dimensions (n rows and 4 columns). Care should be taken so that four adjacent bits in the input data (forming one symbol) are placed in four different columns. For this purpose we first divide the array into a four-row matrix with n columns and then take its transpose. This matrix is multiplied by a 4x1 matrix . This will yield a 1xn column matrix of n symbols (binary to decimal conversion).

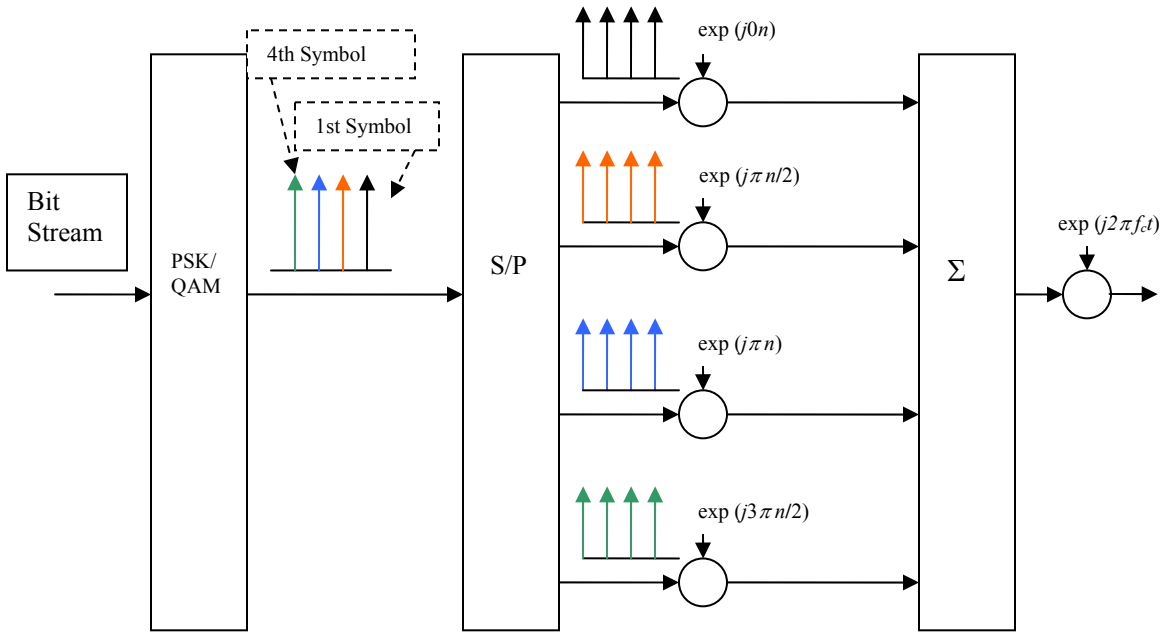

Figure 1.3: A 4-subcarrier OFDM transmitter [4]

In the next step of symbol mapping each symbol is assigned a phase using PSK. The array of symbols generated by symbol mapping process is incremented by 1 so that each element of the array gets incremented to the range of 1 to 2M from 0 to 2M -1. Where M=4 for quadrature. Now each symbol is assigned a phase from a look up table of different equally spaced phases. The look up table phases is made keeping in mind the gray code sequence so that after assigning of phases we get a matrix containing phases, each phase corresponding to a specific symbol in the range of 1 to 2M. The phases are assigned to the symbols from the lookup table in such a way that each phase index corresponds to symbol value. Here gray coding is used because in gray code there is only one bit change between two consecutive codes, so if a symbol is wrongly detected, gray coding makes sure that error is of only one bit.

1.3.2 Serial to Parallel

After assigning phases to each matrix element we get a serial array of PSK symbols. For OFDM we take IFFT of the data in order to transmit data over many sub-carriers. But the problem is that IFFT is taken on parallel streams of data. We convert the serial array

{1x (no. of symbols x FFT size)} into an "FFTsize x N" matrix, where N is the number of symbols and FFTsize is the number of sub-carriers modulated by each symbol. The symbols are then used to map sub-carriers amplitude and phase.

1.4 Intersymbol and Intercarrier Interference

In a multipath environment, a transmitted symbol takes different times to reach the receiver through different propagation paths. From the receiver's point of view, the channel introduces time dispersion in which the duration of the received symbol is stretched. Extending the symbol duration causes the current received symbol to overlap previous received symbols and results in intersymbol interference (ISI). In OFDM, ISI usually refers to interference of an OFDM symbol by previous OFDM symbols.

In OFDM, the receiver samples data symbols on individual subcarriers at the maximum of the subcarrier and demodulates them free from any interference from the other subcarriers (interchannel interference).

The orthogonality of a subcarrier with respect to other subcarriers is lost if the subcarrier has non-zero spectral value at other subcarrier frequencies. From the time domain perspective, the corresponding sinusoid no longer has an integer number of cycles within the FFT interval. Figure 1.5 shows the spectra of four subcarriers in the frequency domain when orthogonality is lost. ICI occurs when the multipath channel varies over one OFDM symbol time [7]. When this happens, the Doppler shifts on each multipath component cause a frequency offset on the subcarriers, resulting in the loss of orthogonality among them. ICI also occurs when an OFDM symbol experiences ISI.

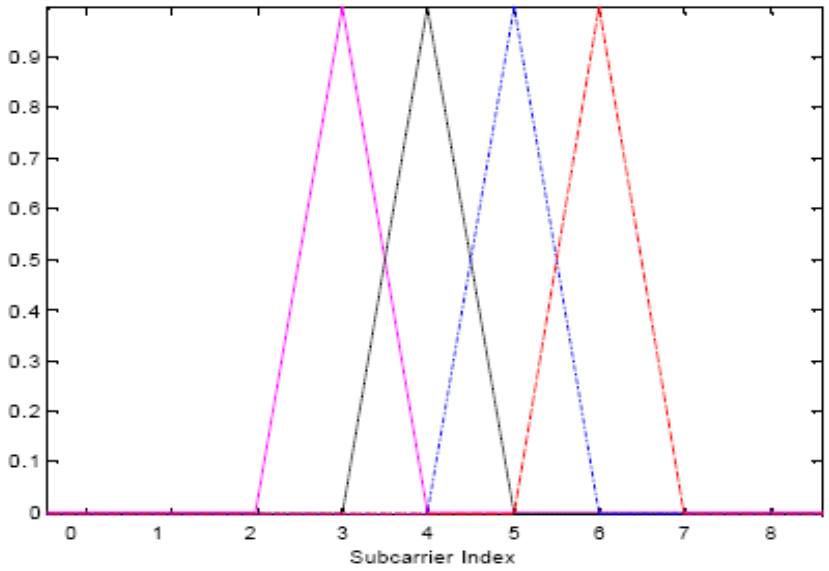

Figure 1.4: Spectra of four orthogonal subcarriers [7]

This situation can be viewed from the time domain perspective, in which the integer number of cycles for each subcarrier within the FFT interval of the current symbol is no longer maintained due to the phase transition introduced by the previous symbol. Finally, any offset between the subcarrier frequencies of the transmitter and receiver also introduces ICI to an OFDM symbol.

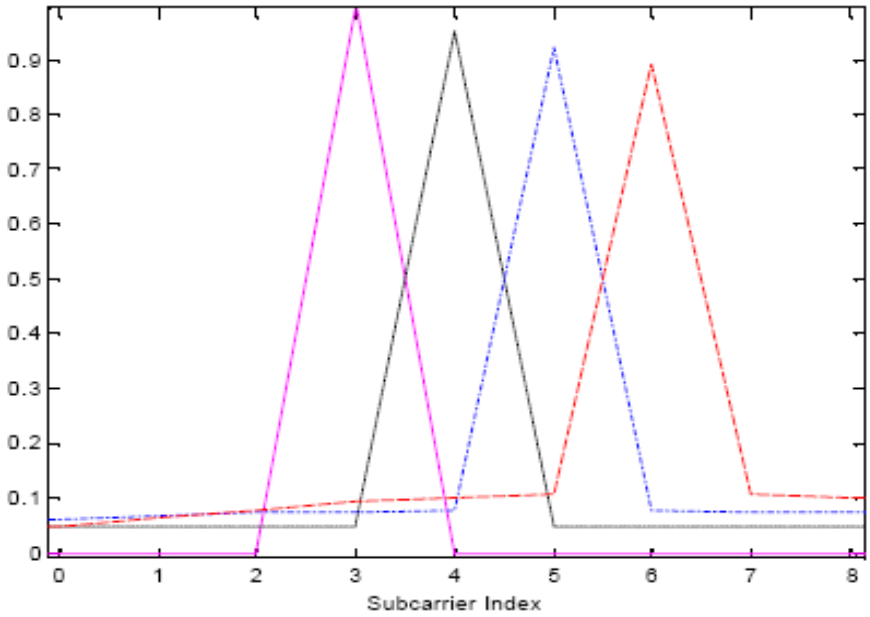

Figure 1.5: Spectra of four non-orthogonal subcarriers [7]

1.5 Guard Time Insertion

OFDM is resilient to ISI because its symbol duration is long compared with the data symbols in the serial data stream. For an OFDM transmitter with N subcarriers, if the duration of a data symbol is T', the symbol duration of the OFDM symbol at the output of the transmitter is

$$T_{sym} = T'N \tag{1.2}$$

Thus if the delay spread of a multipath channel is greater than T' but less then T_{sym}, the data symbol in the serial data stream will experience frequency-selective fading while the data symbol on each subcarrier will experience only flat-fading. Moreover, to further reduce the ISI, a guard time is inserted at the beginning of each OFDM symbol before transmission and removed at the receiver before the FFT operation. If the guard time is chosen such that its duration is longer than the delay spread, the ISI can be completely eliminated. Figure 1.6 illustrates the concept of guard time insertion to eliminate ISI for an OFDM symbol. In Figure 1.6(a), an OFDM symbol received from the first path is interfered by the previous OFDM symbol received from the second and third paths. On the other hand, Figure 1.6(b) shows that the OFDM symbol received from the first path is no longer interfered by the previous OFDM symbol. However, the received symbol is still interfered by its replicas and we refer to this type of interference as self-interference.

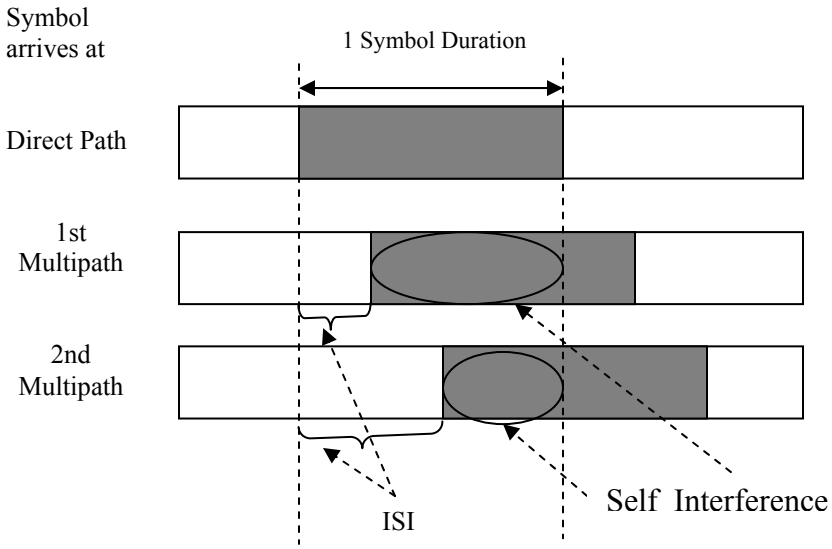

Figure 1.6(a): Received OFDM symbols after passing through a multipath channel without guard time [4]

In order to preserve orthogonality among subcarriers, the guard time is inserted by cyclically extending an OFDM symbol. This ensures that delayed replicas of the OFDM symbols always have an integer number of cycles within the FFT interval. If the delay spread is less than the guard time, the delay spread only introduces a different phase shift for each subcarrier but does not destroy the orthogonality between subcarriers. Guard time insertion can be performed by extracting a portion of an OFDM symbol at the end and appending it to the beginning of the OFDM symbol. Samples after guard time insertion can be expressed as [6]

$$x_k^g = x_{(k+N-G)_N}, \quad 0 \le k \le N+G-1 \tag{1.3}$$

where k is the sample index of an OFDM symbol, N is the number of subcarriers, G is the guard time duration, and $(k)N$ is the residue modulo N.

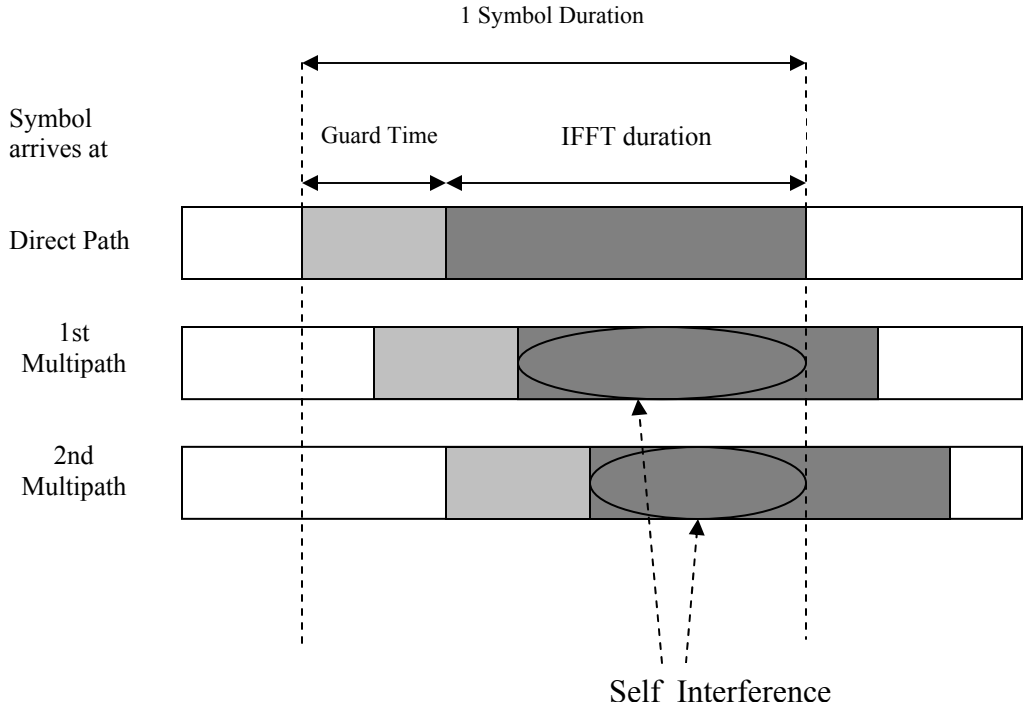

Figure 1.6(b): Received OFDM symbols after passing through a multipath channel with guard time [4]

For the same guard time duration, this method gives the maximum delay spread tolerance since the whole guard time is contributed to eliminate ISI.

1.6 OFDM Receiver

At the receiving end we do the inverse of the process done at the transmitting end. First we use coherent demodulation technique, then remove the cyclic extension and input the serial data to serial to parallel converter. Then we use FFT to separate the sub-carriers and convert the parallel data in to serial data using parallel to serial converter. Finally using the lookup table we extract the data bits that were transmitted.

1.7 Chapter Summary

In this chapter, we introduced the basic concept of OFDM, starting from the concept of orthogonality. Then we moved on to the generation of OFDM symbols. The OFDM modulation and demodulation process was explained, along with important concepts including ISI, ICI, guard time and a brief working of the OFDM receiver at the end.

CHAPTER 2: FUNDAMENTALS OF ANTENNA ARRAYS

2.1 Antenna Arrays

An antenna Array is a configuration of individual radiating elements that are arranged in space and can be used to produce a directional radiation pattern. Single-element antennas have radiation patterns that are broad and hence have a low directivity that is not suitable for long distance communications. A high directivity can still be achieved with single-element antennas by increasing the electrical dimensions (in terms of wavelength) and hence the physical size of the antenna. When increasing the electrical size of an antenna is not possible, high directivity can be achieved by using multiple antenna elements that are spatially arranged in a geometric configuration and electrically connected [8]. These configurations are called antenna arrays and are available as linear array, circular array, and planar array. The elements of the antenna array can contain any number of different antenna apertures (i.e. dipoles, loops, corner reflectors, horns, etc.) but it is practical to use identical elements in an array to provide a convenient and simple means for analysis.

2.1.1 Linear Arrays

When an antenna array has elements arranged in a straight line it is known as a linear array. The radiating pattern of the array depends on the configuration, the distance between the elements, the amplitude and phase excitation of the elements, and also the radiation pattern of individual elements. Figure 2.3 shows a uniformly spaced linear array.

2.1.2 Planar Arrays

An antenna configuration in which all the elements are in one plane is called a planer array. A planar array provides a large aperture and may be used for directional beam control by varying the relative phase of each element. Figure 2.1 shows an NxM element planar array.

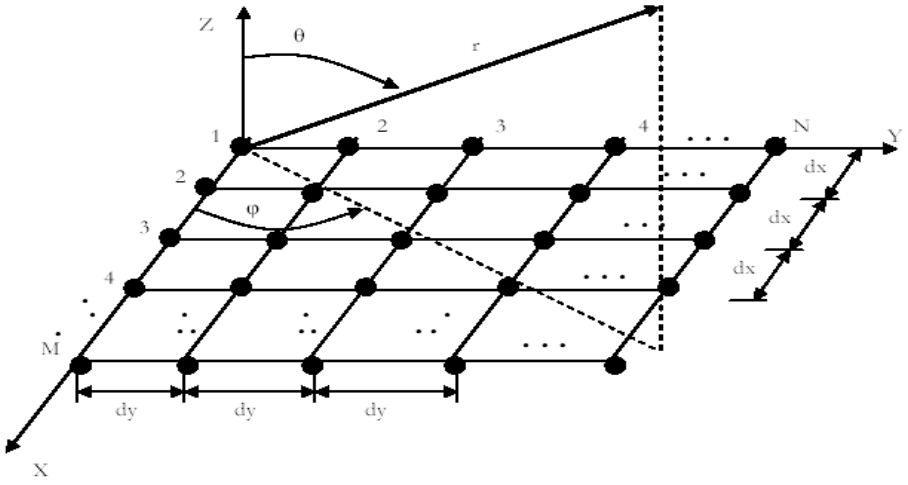

Figure 2.1: NxM element planar array [8]

2.1.3 Circular Array

In this configuration, all antenna elements are distributed along a circle. A circular array is a special form of planar array in which the antennas are located on a horizontal plane in a circular fashion.

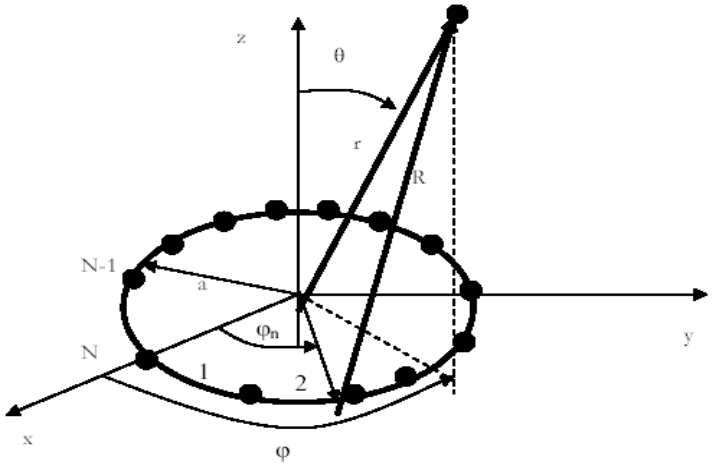

Figure 2.2: N element circular array [8]

The simulation in this project was done for a uniformly spaced linear array.

2.2 Uniformly Spaced Linear Array

Figure 2.3 shows a uniformly spaced linear array with *K* identical isotropic elements, with the rightmost element as reference element.

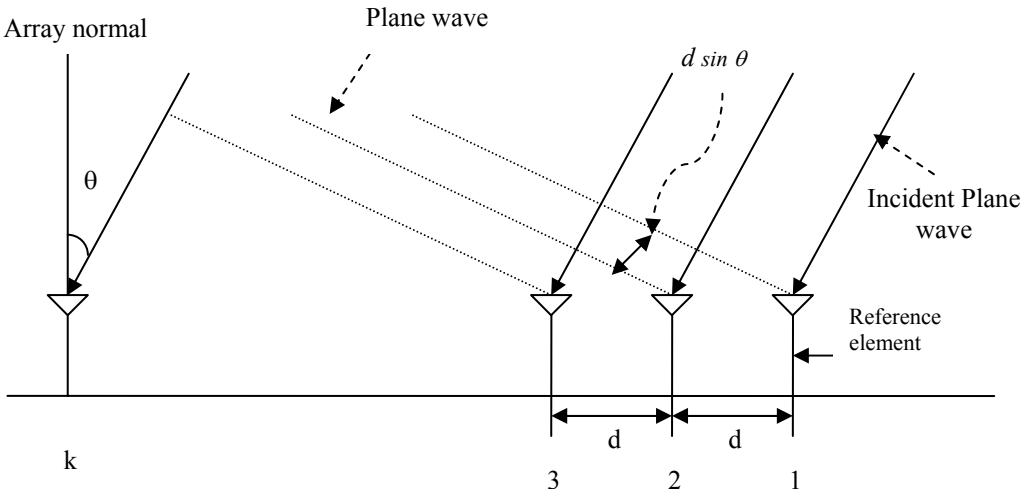

Figure 2.3: A uniformly spaced linear antenna array [4]

A single source is assumed to be transmitting from a far distance so that the received signal at the antenna array is considered to be a plane wave incident at an angle q with respect to the array normal. According to Figure 2.3, the plane wave first reaches the first antenna element, which is the reference element, and propagates all the way to the K-th antenna element.

The received signal at the first antenna element can be expressed as

$$\tilde{x}_1(t) = \mathrm{Re}[x_1(t)\exp\{j2\pi f_c t\}] \tag{2.1}$$

where $x_1(t)$ is the complex envelope representation of the received signal and f_c is the carrier frequency. The propagation delay from the first to second antenna element is

$$\tau = \frac{d\sin\theta}{c} \tag{2.2}$$

where c is the speed of the light. Therefore, the received signal at the second antenna element with respect to the received signal at the first antenna can be expressed as

$$\tilde{x}_2(t = \mathrm{Re}[x_1(t-\tau)\exp\{-j2\pi f_c t\}]) \tag{2.3}$$

If the carrier frequency is large compared with the bandwidth of the signal, the narrowband signal model can be applied here, in which a small time delay can be modeled as a simple phase shift. In this case, equation 2.3 can be rewritten as

$$x_2(t) = \mathrm{Re}[x_1 \exp\{-j2\pi f_c(t-\tau)\}] \tag{2.4}$$

and its complex envelope representation is given by

$$x_2(t) = x_1(t)\exp(-j2\pi f_c \tau) \tag{2.5}$$

Substituting equation 2.2 in 2.5, we have

$$\begin{aligned} x_2(t) &= x_1(t)\exp\left\{-j2\pi f_c \frac{d\sin\theta}{c}\right\} \\ &= x_1(t)\exp\left\{-j\frac{2\rho}{\lambda}d\sin\theta\right\} \end{aligned} \tag{2.6}$$

where λ is the wavelength of the carrier. Since the antenna elements are uniformly distributed across the antenna array, the propagation delay along any two consecutive elements is the same and therefore the complex envelope representation of the received signal at the *k*-th antenna element can be expressed as

$$x_k(t) = x_1(t)\exp\left\{-j\frac{2\pi}{\lambda}(k-1)d\sin\theta\right\}, k = 1,...,K \tag{2.7}$$

The received signal can also be expressed in terms of vector notation as:

$$x(t) = \left[x_1(t), x_2(t),..., x_k(t)\right]^T \tag{2.8}$$

$$a(\theta) = \left[1, e^{-j\frac{2\pi}{\lambda}d\sin\theta},..., e^{-j\frac{2\pi}{\lambda}(K-1)d\sin\theta}\right]^T \tag{2.9}$$

where a(Θ) is known as the array response vector or the steering vector.

2.3 Array Response for Linear Array

The array response vector in equation 2.9 represents the case in which each antenna element is isotropic. The term "isotropic" means that each antenna element can radiate or receive energy uniformly in all directions. In practice, antenna elements usually have non-uniform radiation patterns. One needs to perform array calibration to determine the array response vector for a range of angles and carrier frequencies. This can be done by placing a transmitter at various spatial locations and transmitting signals with different frequencies to estimate the array response vector of the antenna array. For a group of antenna elements that have similar but non-isotropic radiation pattern, the array beam pattern can be calculated based on the principle of pattern multiplication [9] as:

$$G(\theta) = f(\theta)F(\theta) \tag{2.10}$$

where f (Θ) is the radiation pattern for a set of antenna elements that have similar radiation pattern and F (Θ) is the array factor. The array factor is discussed in detail in subsequent chapters.

2.4 Antenna Array as Spatial Filter

A transmitted signal is distorted when it travels through a non-ideal channel. A non-ideal channel is the one that does not have constant amplitude and linear phase response [3]. A filter is implemented at the receiver to extract information from this distorted signal. For example, a time-dispersive channel is a non-ideal channel which stretches a transmitted signal in time and causes ISI. A temporal filter, also known as a time-domain equalizer, is used to compensate the time-dispersive nature of the channel [3]. Time-dispersion implies frequency-selective fading and thus a frequency-domain equalizer can be used as the counterpart of the time-domain equalizer to compensate the frequency-selective nature of the channel [13]. On the other hand, a spatial filter collects a set of data over a spatial aperture using an antenna array and combines them based on a certain criterion to separate the desired signal from the interfering signals having the same frequency content but originating from different spatial locations. This process is known as beamforming [3].

2.5 Element Spacing

A spatial filter can be considered as the counterpart of a temporal filter to extract the desired signal from interfering signals, with one operating in the spatial domain and the other one in the time domain [10]. For a narrowband beamformer, an intense mathematical treatment given in [11] results in the following observations:

1. The normalized element spacing (d / λ) of the spatial filter corresponds to the sampling period T_s of the temporal filter.
2. The sine of the Angle of arrival (AOA) Θ_i, , sin Θ_i , of the spatial filter corresponds to the temporal frequency f_k of the temporal filter input

According to the Nyquist sampling theorem [12], in order to avoid aliasing, the sampling frequency of the temporal filter must be at least twice the highest frequency of the input signal. Since there is a correspondence between the temporal filter and the spatial filter, a corresponding theorem, named spatial Nyquist sampling theorem, is applied to the spatial filter. In the spatial domain, since λ / d corresponds to the sampling frequency of the temporal filter, and the highest frequency corresponds to 1 (since the largest value for $\sin\Theta_i$ is 1), the spatial Nyquist sampling theorem states that

$$\frac{\lambda}{d} \geq 2 \times 1 \tag{2.11}$$

or equivalently,

$$d \leq \frac{\lambda}{2} \tag{2.12}$$

That is, the spacing between two antenna elements should be less than or equal to a half wavelength of the input signal in order to avoid aliasing. Spatial aliasing corresponds to an ambiguity in source locations. This means that the array response vectors for two different angles are the same, i.e.

$$a(\theta_1) = a(\theta_2), where \theta_1 = \theta_2 \tag{2.13}$$

Even though the antenna spacing satisfies the spatial Nyquist sampling theorem, equation 2.13 can still happen when $\Theta_2 = \pi - \Theta_1$, since $\sin\theta = \sin(\pi - \Theta)$. This type of ambiguity is

referred to as array ambiguity. Array ambiguity happens in the uniformly spaced linear array but not in the non-linear spacing array such as the circular array. Antenna spacing larger than a half wavelength causes aliasing; on the other hand, small antenna spacing not only reduces spatial discrimination because of the ill-dispersed of the array response vectors in the N dimensional vector space but also causes mutual coupling effects [14]. In practice, the antenna spacing is often kept near a half wavelength so that the spatial aliasing is avoided and the mutual coupling effect is minimized.

CHAPTER 3: ADAPTIVE ANTENNA SYSTEMS

Adaptive antenna is one of the most promising technologies that will enable a higher capacity in wireless networks by effectively reducing multipath and inter-channel interference [15]. This is achieved by focusing the radiation only in the desired direction and adjusting itself to changing traffic conditions or signal environments. Adaptive antennas employ a set of radiating elements arranged in the form of an array. The signals from these elements are combined to form a movable or switchable beam pattern that follows the desired user. In an adaptive antenna system the arrays by themselves are not adaptive; it is the digital signal processing that makes them adaptive. The process of combining the signals and then focusing the radiation in a particular direction is often referred to as digital beamforming [17], [18].

The early adaptive antenna systems were designed for use in military applications to suppress interfering or jamming signals from the enemy [19]. Since interference suppression was a feature in this system, this technology was borrowed to apply to personal wireless communications where interference was limiting the number of users that a network could handle. It is a major challenge to apply adaptive antenna technology to personal wireless communications since the traffic is denser. Also, the time available for complex computations is limited. However, the advent of powerful, low-cost, digital processing components and the development of software-based techniques have made adaptive antenna systems a practical reality for wireless communications systems.

3.1 Adaptive Array Systems

Great performance improvements can be achieved by implementing advanced signal processing techniques to process the information obtained by the antenna arrays. The adaptive array systems are really smart because they are able to dynamically react to the changing RF environment. They have a multitude of radiation patterns compared to fixed finite patterns in switched beam systems to adapt to the ever-changing RF environment.

An adaptive array, like a switched beam system uses antenna arrays but it is controlled by signal processing. This signal processing steers the radiation beam towards a desired mobile user, follows the user as he moves, and at the same time minimizes interference arising from other users by introducing nulls in their directions. This is illustrated in a simple diagram shown below in figure 3.1

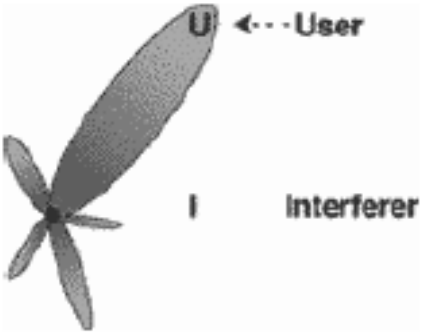

Figure 3.1 Beam formation for adaptive array antenna system [20]

The smartness in these systems comes from the intelligent digital processor that is incorporated in the system. The processing is mainly governed by complex computationally intensive algorithms.

3.1.1 Basic Working Mechanism

An adaptive antenna system can perform the following functions: Firstly, the direction of arrival of all the incoming signals including the interfering signals and the multipath signals are estimated. Secondly, the desired user signal is identified and separated from the rest of the unwanted incoming signals. Lastly a beam is steered in the direction of the desired signal and the user is tracked as he moves while placing nulls at interfering signal directions by constantly updating the complex weights.

As discussed previously in the chapter of arrays it is quite evident that the direction of radiation of the main beam in an array depends upon the phase difference between the elements of the array. Therefore it is possible to continuously steer the main beam in any direction by adjusting the progressive phase difference between the elements. The same concept forms the basis in adaptive array systems in which the phase is adjusted to achieve maximum radiation in the desired direction. To have a better understanding of

how an adaptive array system works, let us consider a typical adaptive digital beamforming network shown in figure 3.2:

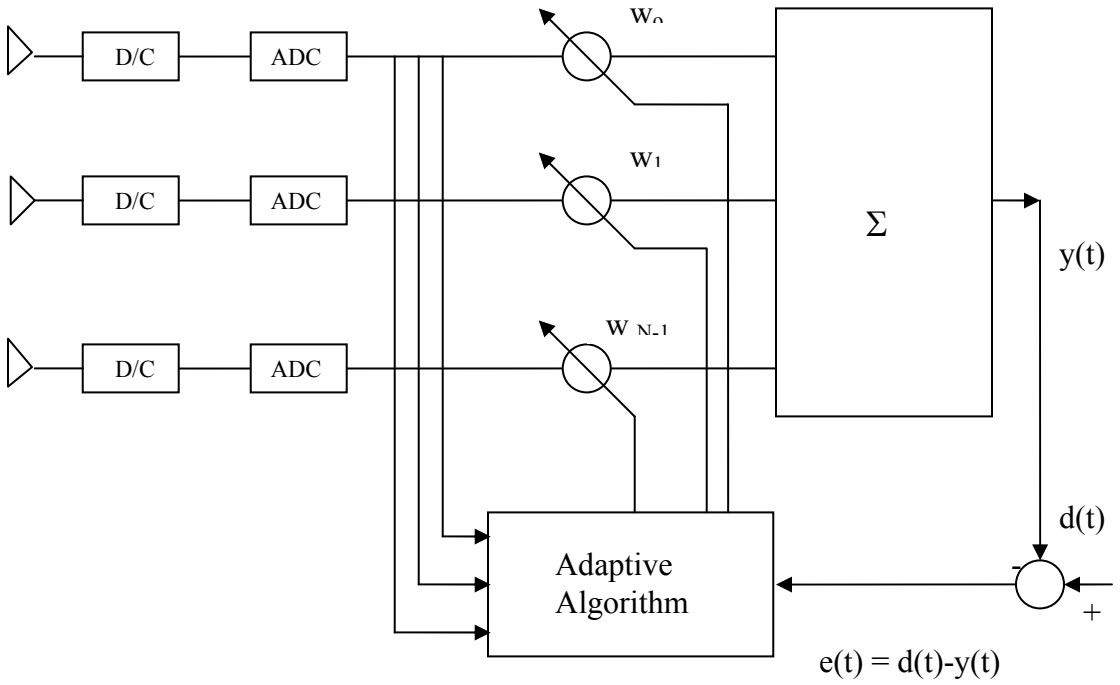

Figure 3.2: Block diagram of Adaptive array systems [20]

In a beamforming network typically the signals incident at the individual elements are combined intelligently to form a single desired beamformed output. Before the incoming signals are weighted they are brought down to baseband frequencies. The receivers provided at the output of each element perform the necessary frequency down conversion. Adaptive antenna array systems use digital signal processors (DSPs) to weigh the incoming signal. Therefore it is required that the down-converted signal be converted into digital format before they are processed by the DSP. Analog-to-digital converters (ADC's) are provided for this purpose. For accurate performance, they are required to provide accurate translation of the RF signal from the analog to the digital domain. The digital signal processor forms the heart of the system, which accepts the baseband signal in digital format and the processing of the digital data is driven by software. The processor interprets the incoming data information, determines the complex weights (amplification and phase information) and multiplies the weights to each element output to optimize the array pattern. The optimization is based on a particular criterion, which

minimizes the contribution from noise and interference while producing maximum beam gain at the desired direction. There are several algorithms based on different criteria for updating and computing the optimum weights.

3.2 Multipath

In wireless communication systems, capacity and performance are usually limited by two major impairments. They are multipath and inter-channel interference [4]. Multipath is a condition which arises when a transmitted signal undergoes reflection from various obstacles in the propagation environment. This gives rise to multiple signals arriving from different directions. Since the multipath signals follow different paths, they have different phases when they arrive at the receiver. The result is degradation in signal quality when they are combined at the receiver due to the phase mismatch. Inter-channel interference is the interference between two signals that operate at the same frequency. Beamforming is used to suppress both multipath effects as well as inter-channel interference caused by jamming signals. Jamming signals are transmitted at the same frequency and at much higher power than desired signal.

3.3 Beamforming

The objective of beamforming is to separate the desired signal from interfering signals, given that they have the same frequencies but different spatial locations. Interfering signals can be the delayed version of the desired signal originated from the multipath environment or signals generated by other users. A digital beamformer samples the propagated wave field at the input of each antenna element, weights them based on a certain performance criterion and then combines them at the output of the beamformer.

3.3.1 Narrowband Beamformer

Figure 3.3 shows a narrowband beamformer. A narrowband signal sampled at the *k*-th antenna element at time *n* is just the phase-shifted version of the signal received at the reference antenna element at time *n*. Since this phase shift is a function of the distance between the first antenna element and the *k*-th antenna element, a narrowband beamformer needs to sample the propagating wave field in space only. The signal at the

output of the beamformer at time *n*, *y(n)*, is given by a linear combination of the data at the *K* elements at time *n*.

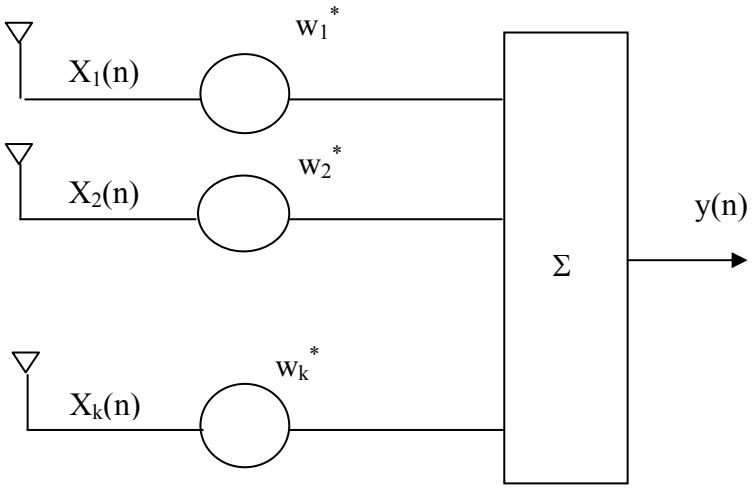

Figure 3.3 A narrowband beamformer [4]

$$y(n) = \sum_{k=1}^{K} w_k^* x_k(n) \tag{3.1}$$

where * represents the complex conjugate, $x_k(n)$ is the complex envelope representation of the received signal from the *k*-th antenna element at time *n*, and w_k is the complex weight applied to $x_k(n)$. Equation 3.1 can be represented in vector form as

$$y(n) = w^H x(n) \tag{3.2}$$

where *H* denotes the Hermitian (complex conjugate) transpose and

$$w = \left[w_1, w_2, ..., w_k\right]^T \tag{3.3}$$

is the complex weight vector. Each antenna element is assumed to have any necessary receiver electronics and an Analog to Digital (A/D) converter if beamforming is performed digitally.

3.3.2 Wideband Beamformer

For wideband signals, a different approach has to be taken. A wideband signal sampled at the k-th antenna element at time *n* is not only a phase shift but also time delayed with respect to the signal received at the reference antenna element sampled at time *n*. This requires a wideband beamformer to sample the propagating wave field in both space and time. Figure shows a wideband beamformer.

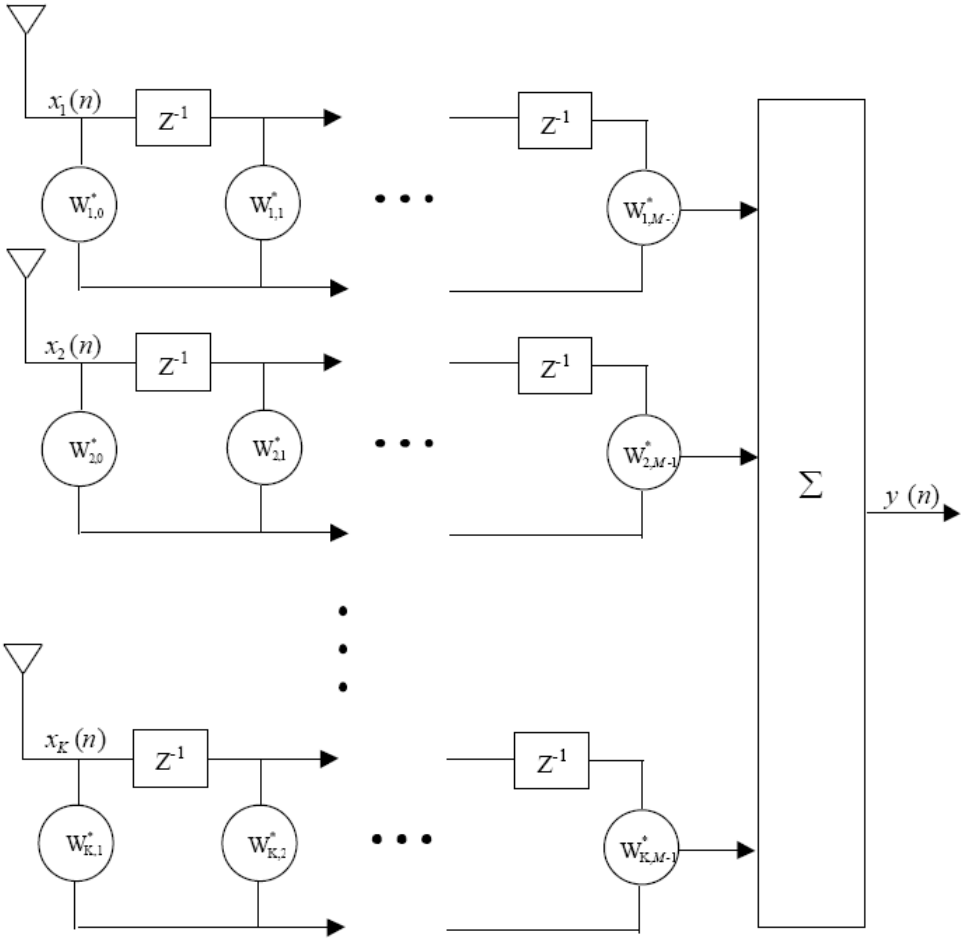

Figure 3.4: A wideband beamformer [4]

To reduce the number of beamformers used, and hence reduce complexity of the system, beamformer can be implemented in the frequency domain. In frequency domain beamforming, a group of subcarriers can be handled by a single beamformer.

3.4 Frequency-domain Beamforming

A frequency-domain beamformer first accumulates the sampled signal at each antenna element to form *N*-point data blocks. It then takes an *N*-point Discrete Fourier Transform of the data at each antenna element using the Fast Fourier Transform (FFT) algorithm and performs beamforming on individual frequency components to accommodate different phase shifts experienced by each of them. At the output of the beamformer, an *N*-point Inverse Discrete Fourier Transform is performed to convert the data back to the time domain. By proper selection of beamformer weights and careful data partitioning, the frequency domain beamformer output is equivalent to the wideband beamformer output.

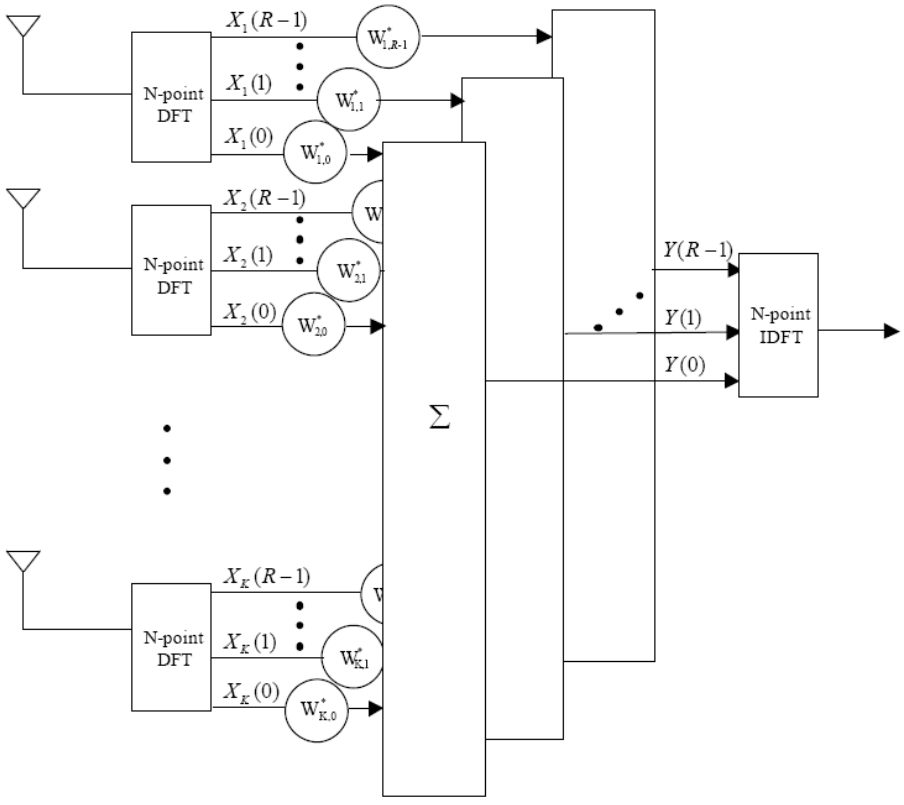

Figure 3.5 : Frequency Domain Beamformer [4]

3.5 Frequency-domain Beamforming in OFDM

The frequency-domain beamforming allows an OFDM receiver to bypass equalization, since the weight vector of individual beamformers will attempt to minimize the effect of the multiplicative distortion associated with the demodulated symbols on individual subcarriers. This gives a big advantage because one needs to estimate the channel frequency response in order to perform equalization, and in the interference environment where the interference power is higher than the power of the desired signal, it is difficult to estimate the channel frequency response for the desired user. Thus, the frequency-domain beamforming scheme avoids the channel estimation problem under the interference environment. Having individual beamformers to process its own subcarriers is also an advantage for suppressing the narrowband interference. Narrowband interference corrupts only a portion of the signal bandwidth. Having multiple beamformers across the signal bandwidth provides flexibility so that individual beamformers are able to adjust their own weights to adapt different interference patterns that may be experienced by different subcarriers simultaneously.

The *m*-th sample of an OFDM symbol at the output of an OFDM transmitter can be written as:

$$x_m = \sum_{n=0}^{N-1} X_n \exp\left\{ j \frac{2\pi mn}{N} \right\}, 0 \le m \le N-1 \tag{3.4}$$

where N is the number of subcarriers and X_n is the data symbol on the n-th subcarrier. We assume that each OFDM symbol is transmitted through a multipath channel with L discrete paths and the receiver deploys a uniformly spaced linear array consists of K elements. Using the narrowband model assumption, the m-th sample at the k-th antenna element can be written as:

$$r_{m,k} = \sum_{l=0}^{L-1} h_{m,l} x_m \exp\left\{ - j\left(\frac{2\pi}{\lambda}(k-1)d\sin\theta\right) \right\} + n_{m,k}, 0 \le m \le N-1 \tag{3.5}$$

where d is the antenna spacing, λ is the wavelength of the carrier, θ is the AOA with respect to the array normal, $h_{m,l}$ is the complex random variable for the l-th path of the channel impulse response at time m, and $n_{m,k}$ is the AWGN at the k-th antenna element at time m. If we let $w_k(\theta)$ be the phase shift of the received signal at the k-th antenna element with respect to the received signal at the reference antenna element, equation 3.5 can be written as

$$r_{m,k} = \sum_{l=0}^{L-1} h_{m,l} x_m \exp\{-jw_k(\theta)\} + n_{m,k}, 0 \le m \le N-1 \tag{3.6}$$

where,

$$w_k(\theta) = \frac{2\pi}{\lambda}(k-1)d\sin\theta \tag{3.7}$$

We assume that the guard time is longer than the delay spread so that ISI can be completely eliminated. The demodulated symbol on the n-th subcarrier at the output of FFT at the k-th antenna element can be written as [35]

$$\begin{aligned} Y_{n,k} &= \sum_{m=0}^{N-1}\sum_{l=0}^{L-1} X_m H_l(n-m)\exp\left\{-j\left(\frac{2\pi ml}{N} + w_k(\theta)\right)\right\} + N_{m,k} \\ &= \left[\sum_{l=0}^{L-1} H_l(0)\exp\left\{-j\left(\frac{2\pi ml}{N} + w_k(\theta)\right)\right\}\right] X_n + \sum_{m=0}^{N-1}\sum_{l=0}^{L-1} X_m H_l(n-m)\exp\left\{-j\left(\frac{2\pi ml}{N} + w_k(\theta)\right)\right\} \\ &+ N_{n,k} \\ &= a_{n,k} X_n + \beta_{n,k} + N_{n,k}, 0 \le n \le N-1 \end{aligned} \tag{3.8}$$

where $N_{n,k}$ is the AWGN on the n-th subcarrier at the k-th antenna element, $a_{n,k}$ is the multiplicative distortion caused by the channel at the desired subcarrier at the k-th antenna element, $\beta_{n,k}$ is the ICI term, and $H_l(n-m)$ is the FFT of a time-variant multipath channel $h_{m,l}$ which is defined as follows:

$$H_l(n-m) = \frac{1}{N}\sum_{k=0}^{N-1} h_{m,l}\exp\left\{-j\frac{2\pi k(n-m)}{N}\right\} \tag{3.9}$$

If we assume the multipath channel is time-invariant over one OFDM symbol duration, $H_l\ (n\text{-}m)$ in equation 3.9 becomes zero and thus there is no ICI and, $\square_{n,k}$ $\tilde{\square}$ in equation 3.8. The multiplicative distortion $a_{n,k}$ in equation 3.8 can be eliminated by using a one-tap equalizer at the n-th subcarrier. However, $a_{n,k}$ contains $\square_k\ (w)$, which provides the Angle of Arrival information for beamforming. Thus equalization should not be performed in order to keep the AOA information. Instead, we leave the multiplicative distortion with the demodulated symbol and pass it to the beamformer so that it can steer the beam towards the direction of the desired user. Using the MMSE criterion, the beamformer should be able to minimize the effect of $a_{n,k}$ when the adaptive beamforming algorithm converges. Since the multiplicative distortion may be fairly distinctive across the subcarriers, a single beamformer with one set of weight vector will not be able to suppress the distortion across them effectively. Therefore, symbols on individual subcarriers should be processed by their own beamformers. In this way, each beamformer has its own set of weight vector which combines the demodulated symbols on its corresponding subcarrier in an optimal way. Figure 3.6 shows the structure of the OFDM receiver using the frequency-domain beamforming approach.

After the FFT operation on each antenna element, demodulated symbols on each subcarrier are passed to the corresponding beamformers. The output of the n-th beamformer can be written as

$$P_n = \sum_{k=1}^{K} W_{n,k}^{*} Y_{n,k}, 0 \le n \le N-1 \tag{3.10}$$

where $W_{n,k}$ is the weight on the k-th antenna element for the n-th beamformer and $Y_{n,k}$ is the demodulated symbol on the n-subcarrier at the k-th antenna element defined in equation 3.8. Parallel-to-serial conversion is performed at the output of beamformers followed by symbol demodulation and decoding.

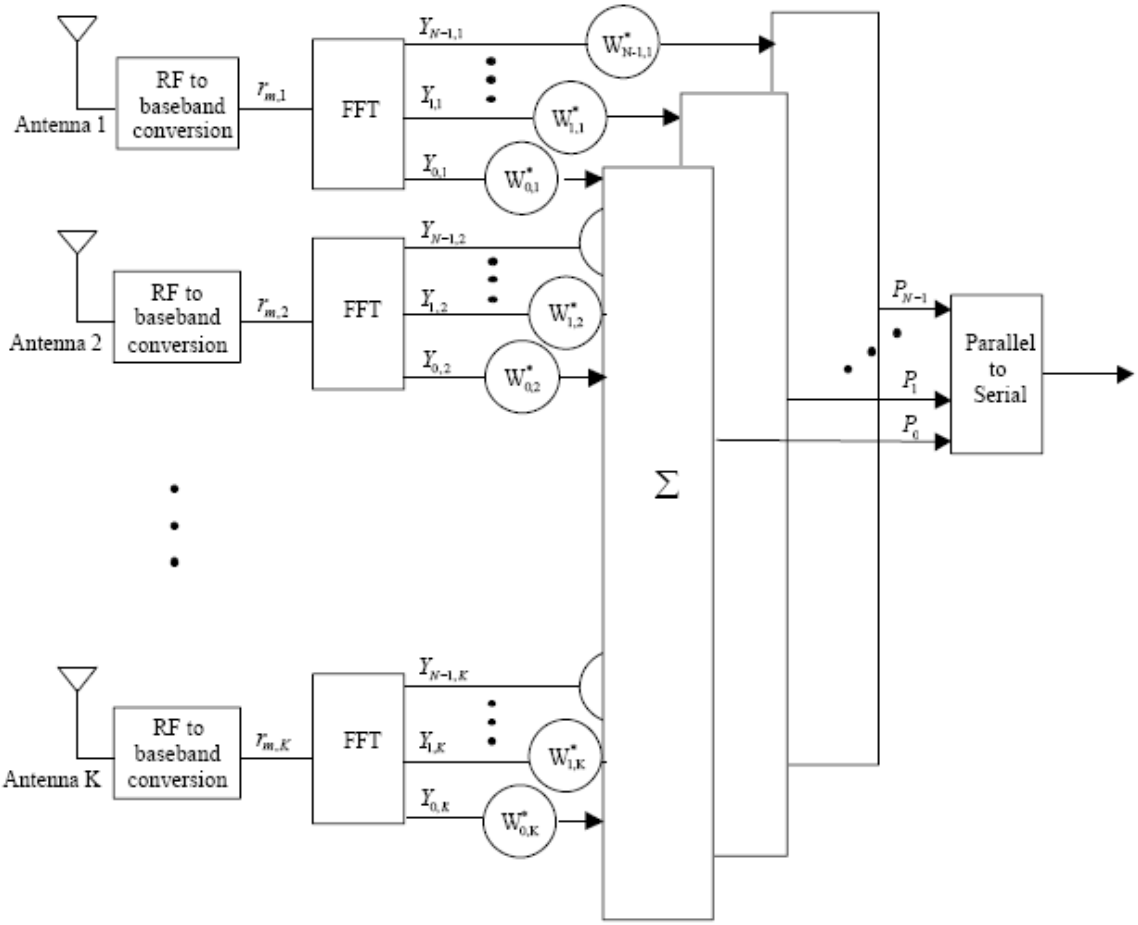

Figure 3.6: The structure of an OFDM receiver using the frequency-domain beamforming approach. [4]

3.6 Benefits of Adaptive Antenna Systems

3.6.1 Reduction in inter-channel interference

Adaptive antennas have a property of spatial filtering to focus radiated energy in the form of narrow beams only in the direction of the desired mobile user and no other direction. In addition they also have nulls in their radiation pattern in the direction of other mobile users in the vicinity. Therefore there is often negligible inter-channel interference.

3.6.2 Range improvement

Since adaptive antennas employ collection of individual elements in the form of an array they give rise to narrow beam with increased gain when compared to conventional

antennas using the same power. The increase in gain leads to increase in range and the coverage of the system. Therefore fewer base stations are required to cover a given area.

3.6.3 Increase in capacity

Adaptive antennas enable reduction in inter-channel interference, which leads to increase in the frequency reuse factor. That is adaptive antennas allow more users to use the same frequency spectrum at the same time bringing about tremendous increase in capacity.

3.6.4 Reduction in transmitted power

Ordinary antennas radiate energy in all directions leading to a waste of power. Comparatively adaptive antennas radiate energy only in the desired direction. Therefore, less power is required for radiation at transmitter. Reduction in transmitted power also implies reduction in interference towards other users.

3.6.5 Reduction in handoff [20]

To improve the capacity in a crowded cellular network, congested cells are further broken into micro cells to enable increase in the frequency reuse factor. This results in frequent handoffs, as the cell size is smaller. Using adaptive antennas at the base station, there is no need to split the cells since the capacity is increased by using independent spot beams. Therefore, handoffs occur rarely, only when two beams using the same frequency cross each other.

3.6.6 Mitigation of multipath effects

Adaptive antennas can either reject multipath components as interference, thus mitigating its effects in terms of fading or it can use the multipath components and add them constructively to enhance system performance.

3.6.7 Compatibility [27]

Adaptive antenna technology can be applied to various multiple access techniques such as TDMA, FDMA, and CDMA. It is compatible with almost any modulation method and bandwidth or frequency band.

3.7 Applications of Adaptive Antennas

1. Due to their interference rejection capability in high data rate communication systems, adaptive antennas would be an inherent part of 4G mobile systems.
2. Digital TV broadcasting systems may have adaptive antennas at the RF end.
3. Military communication may heavily rely on adaptive antennas for overcoming jamming capabilities of enemy.
4. Satellite communication can benefit from adaptive antennas to reduce atmospheric losses.

CHAPTER 4: ADAPTIVE ALGORITHMS

In the preceding chapter, an overview of beamforming was studied. While at this point that topic is well understood, it is still not known how to determine the weights necessary for beamforming. In the following discussion, it is desired to study means in which specific characteristics of the received signal incident upon the array (in addition to the spatial separation among users in the environment) can be exploited to steer beams in directions of desired users and nulls in directions of interferers. In particular, the Mean Square Error (MSE) criterion of a particular weight vector will be minimized through the use of statistical expectations, time averages and instantaneous estimates. As well, the distorted constant modulus of the array output envelope due to noise in the environment will be restored. Each of the characteristics described above correspond to adaptive algorithms which can be classified into two categories [25]:

1.) Decision Directed Adaptive algorithms
2.) Blind Adaptive Algorithms.

1. Decision Directed Adaptive algorithms

These types of algorithms are based on minimization of the mean square error between the received signal and the reference signal. Therefore it is required that a reference signal be available which has high correlation with the desired signal. The reference signal is not the actual desired signal, in fact it is a signal that closely represents it or has strong correlation with it [26]. Reference signals required for the above algorithms are generated in several ways. In TDMA every frame consists of a sequence, which can be used as a reference signal [25]. In digital communication, synchronization signals can be used for the same purpose.

Examples: The Least Mean Square (LMS) algorithm and the Recursive Least Square (RLS) algorithm

2. Blind Adaptive algorithms

These algorithms do not require any reference signal information. They themselves generate the required reference signal from the received signal to get the desired signal.

Examples: The Constant Modulus Algorithm (CMA).

4.1 Non-Blind Adaptive Algorithms [32],[33],[34],[35],[36],[37]

As was noted above, non-blind adaptive algorithms require a training sequence, *d(k)*, in order to extract a desired user from the surrounding environment. This in itself is undesirable for the reason that during the transmission of the training sequence, no communication in the channel can take place. This dramatically reduces the spectral efficiency of any communications system. Additionally, it can be very difficult to understand the statistics of the channel in order to characterize a reasonable estimate of *d(k)* needed to accurately adapt to a desired user. With this in mind, the following summarizes the basic concepts of non-blind adaptive algorithms.

4.2 Adaptation Approaches

There are two distinct approaches that have been widely used in the development of various adaptive algorithms [30]. They are the

1. Stochastic approach.
2. Deterministic approach.

Both have many variations in their implementation, leading to a rich variety of algorithms, each with its own desirable features.

4.2.1 Approach based on Wiener filter theory

According to Wiener filter theory, which comes from the stochastic framework, the optimum coefficients of a linear filter are obtained by minimizing its mean square error (MSE). The minimization of MSE requires certain statistics obtained through ensemble averaging, which may not be possible in practical applications. The problem is solved

using ergodicity, so as to use time averages instead of ensemble averages [30]. Furthermore, to come up with simple recursive algorithms, very rough estimates of the required estimate are used. In fact, the least mean square (LMS) algorithm uses instantaneous value of square of error signal as an estimate of the MSE. This very rough estimate of the MSE when used with a small step-size parameter in searching for the optimum coefficients of the Wiener filter, leads to very simple and yet reliable algorithm. Main advantage of LMS algorithm is that its convergence behavior is highly dependent on the power spectral density of the filter input. When the power spectrum of filter input is flat across the whole range of frequencies, LMS converges very fast. However, when some bands have lower signal energy, slow modes of convergence appear. So, to converge fast, LMS requires equal excitation over the whole range of frequencies. This has been solved by dividing the whole bandwidth into a number of subbands and achieving some degree of signal whitening by using power normalization mechanism, prior to applying adaptive algorithm. An effective way of implementing lengthy filters, at a much lower complexity is by using FFT to implement time domain convolutions in the frequency domain.

4.2.2 Method of Least Squares

The algorithms based on Wiener filter theory have their origin in a statistical formulation of the problem. In contrast to this, method of least squares approaches the problem of filter optimization from a deterministic point of view. In least squares method, the performance index is the sum of the weighted error squares for the given data, i.e. a deterministic quantity. A consequence of this method is that algorithms based on this technique generally converge much faster than LMS based algorithms. They are also insensitive to power spectral density of the input signal. The price to be paid is the increased computational complexity and poorer numerical stability. Direct formulation of least squares problem results in a matrix formulation of its solution which can be applied on a block by block basis to incoming signals. This is called block estimation of least squares method, which has some useful applications in linear predictive coding of speech signals [30]. In context of adaptive filters, recursive formulations of the least squares method that update the filter coefficients after the arrival of every sample of input are

preferred. The derivation of the standard RLS algorithm involves the use of a well known result from linear algebra known as the matrix inversion lemma, which is discussed in detail in [29]. Consequently, the implementation of standard RLS algorithm involves matrix manipulations that result in a computational complexity proportional to the square of the filter length.

4.3 Weiner Optimum Solution [32]

Consider the *least mean square* (LMS) adaptive array shown in Figure 4.1. Through a feedback loop the weights, (w_1 , ... , w_N) are updated by the time sampled error signal:

$$e(k) = d(k) - y(k) \tag{4.1}$$

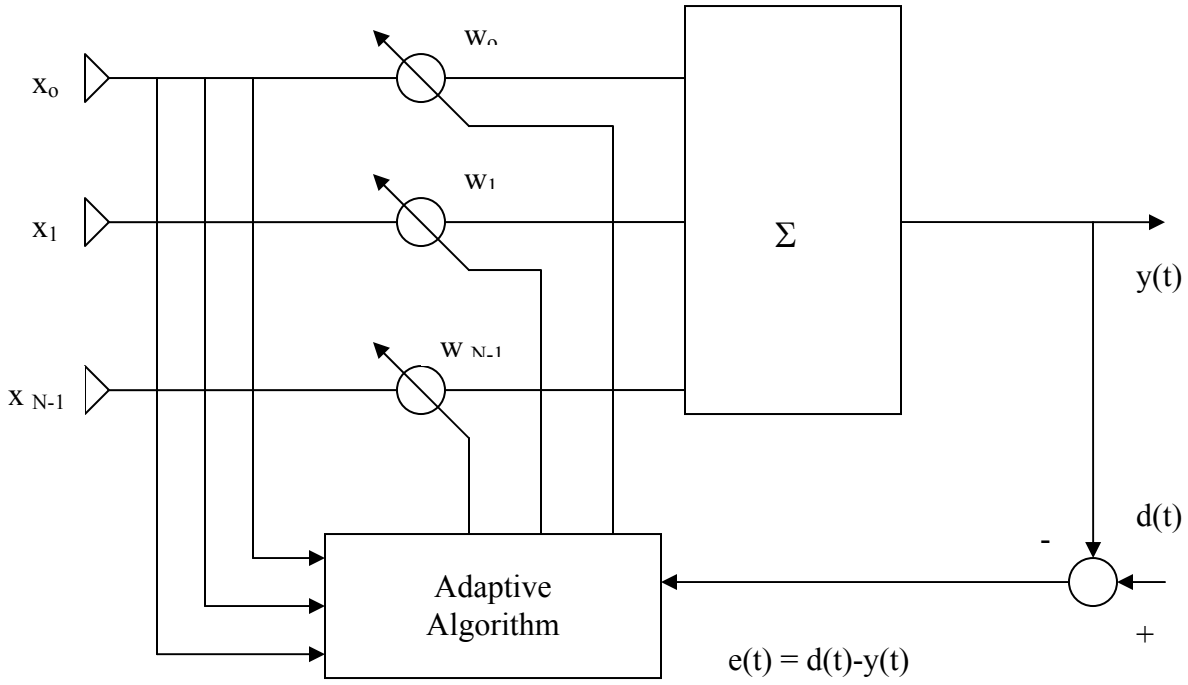

Figure 4.1**:** LMS Adaptive Array [c]

where, the training sequence, *d(k)*, is a near replica of the desired signal and *y(k)* is the output of the adaptive array.

The feedback system attempts to direct the weights at each element to their optimal weights, w_{opt}. The adaptive processor adjusts the weight vector to minimize the mean square error (MSE) of the error signal, *e(k)*, given by:

$$E\left[\left|e(k)\right|^2\right] = E\left[\left|d(k) - y(k)\right|^2\right] \tag{4.2}$$

where, E is the expectation operator.

Substituting equation 3.2 into equation 4.2 and expanding the argument of the MSE term yields:

$$\begin{aligned} E\left[\left|e(k)\right|^2\right] &= E\left[\left\{d(k) - y(k)\right\}\left\{d(k) - y(k)\right\}^*\right] \\ &= E\left[\left\{d(k) - \bar{w}^H \bar{x}(k)\right\}\left\{d(k) - \bar{w}^H \bar{x}(k)\right\}^*\right] \\ &= E\left[\left|d(k)\right|^2 - d(k)\bar{x}^H(k)\bar{w} - \bar{w}^H \bar{x}(k)d^*(k) + \bar{w}^H \bar{x}(k)\bar{w}\right] \end{aligned} \tag{4.3}$$

$$= E\left[\left|d(k)\right|^2 - \bar{\bar{r}}_{xd}^H \bar{w} - \bar{w}^H \bar{r}_{xd} + \bar{w}^H R_{xx} \bar{w}\right] \tag{4.4}$$

where,

$$E\left[\bar{x}(k)\bar{x}^H(k)\right] = R_{xx} \tag{4.5}$$

is the NxN Covariance Matrix of the input data vector, $x(k)$ and

$$E\left[\bar{x}(k)d^*(k)\right] = \bar{\bar{r}}_{xd} \tag{4.6}$$

is the Nx1 Cross-Correlation Vector between the input data vector, $x(k)$, and the training sequence, $d(k)$.

It is apparent from either equation 4.3 or 4.4 that the MSE of the LMS adaptive array is a quadratic function in *w,* where the extremum of this quadratic surface is a unique minimum. By plotting the MSE vs. the weights for equation 4.3, we achieve the following quadratic surface, which is also called the performance surface.

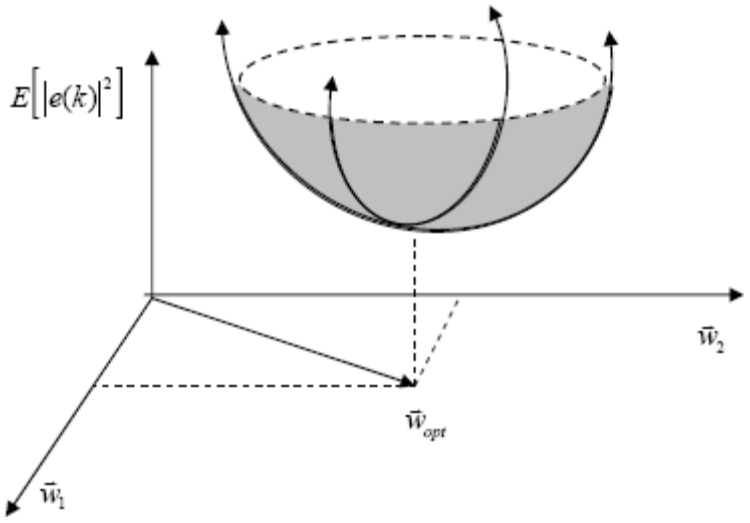

Figure 4.2: Quadratic Surface for MSE criterion of LMS adaptive array [37]

The shape, location, and orientation of the performance surface depicted above depend on the array geometry and the signals incident upon the array. If the incident signals, their AOA's and power are time variant, then the performance surface will move around in space thus altering the value of w_{opt}. It is the job of the adaptive array to force the optimum weight vector to track to the bottom of the surface. The unique minimum of the performance surface can be found by performing the vector gradient operator of the mean square error defined in equation 4.4 with respect to the array weights and setting the result equal to zero.

$$\nabla\left(E\left[|e(k)|^2\right]\right) = \frac{\partial}{\partial \overline{w}^*} E\left[|e(k)|^2\right] = 0 \tag{4.7}$$

which yields,

$$-2\overline{r_{xd}} + 2R_{xx}\overline{w}_{opt} = 0 \tag{4.8}$$

Solving for the optimum weights gives:

$$\overline{w}_{opt} = R_{xx}^{-1}\overline{r}_{xd} \tag{4.9}$$

There exist some disadvantages in using the Weiner Solution to determine the optimum weight vector. In particular, if the number of elements in the linear array is large, then it

is computationally complex to invert the *NxN* covariance matrix, R_{xx}. This is a problem only if the inverse of the covariance matrix is non-singular, which is not always the case. It first would have to be assumed that the matrix is positive semi-definite to begin with in order to use the Weiner solution. Additionally, the Weiner solution requires the use of an expectation operator in both R_{xx} and r_{xd} . This assumes that the statistics of the communications channel and the desired signal estimate, *d(k)*, can be perfectly characterized to produce an adequate training sequence.

4.4 LEAST MEAN SQUARE ALGORITHM (LMS)

4.4.1 Introduction

The Least Mean Square (LMS) algorithm, introduced by Widrow and Hoff in 1959 [38] is an adaptive algorithm, which uses a gradient-based method of steepest decent [25]. LMS algorithm uses the estimates of the gradient vector from the available data. LMS incorporates an iterative procedure that makes successive corrections to the weight vector in the direction of the negative of the gradient vector which eventually leads to the minimum mean square error. Compared to other algorithms LMS algorithm is relatively simple; it does not require correlation function calculation nor does it require matrix inversions.

4.4.2 LMS Algorithm and Adaptive Arrays

Consider a Uniform Linear Array (ULA) with N isotropic elements, which forms the integral part of the adaptive beamforming system as shown in the figure below. The output of the antenna array is given by,

$$x(t) = s(t)a(\theta_0) + \sum_{i=1}^{N_u} u_i(t)a(\theta_i) + n(t) \tag{4.10}$$

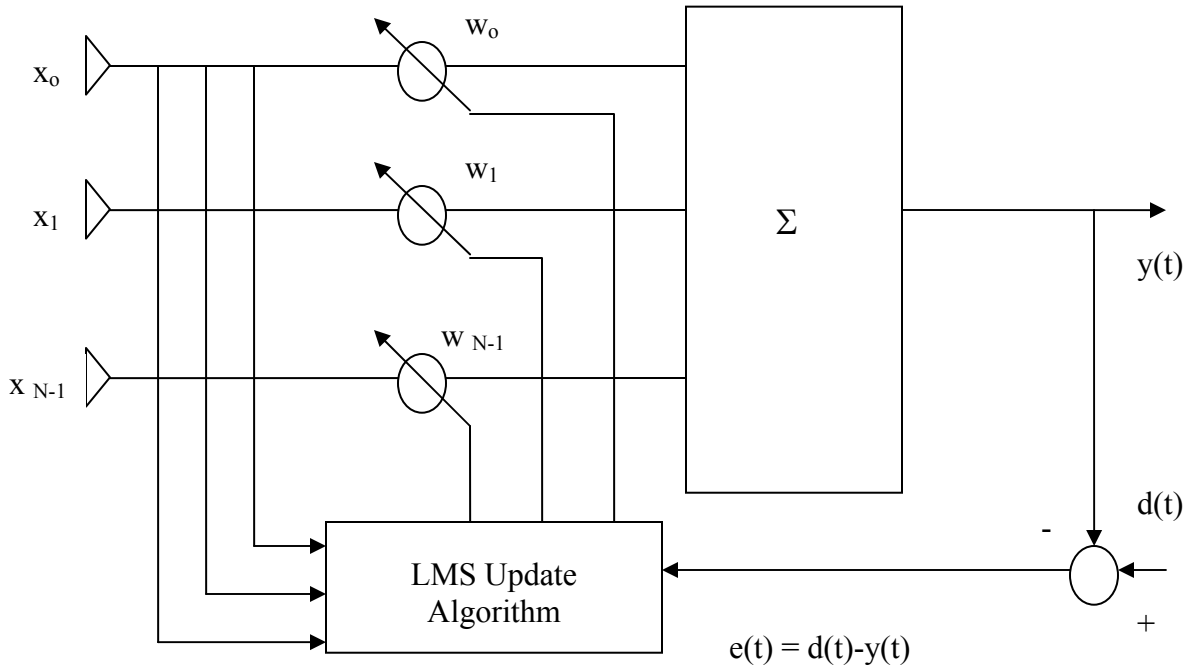

Figure 4.3 LMS adaptive beamforming network [20]

s(t) denotes the desired signal arriving at angle θ_o and $u_i(t)$ denotes interfering signals arriving at angle of incidences θ_i respectively. a(θo) and a(□i) represent the steering vectors for the desired signal and interfering signals respectively. Therefore it is required to construct the desired signal from the received signal amid the interfering signal and additional noise n(t).

As shown above the outputs of the individual sensors are linearly combined after being scaled using corresponding weights such that the antenna array pattern is optimized to have maximum possible gain in the direction of the desired signal and nulls in the direction of the interferers. The weights here will be computed using LMS algorithm based on Minimum Squared Error (MSE) criterion. Therefore the spatial filtering problem involves estimation of signal s(t) from the received signal x(t) (i.e. the array output) by minimizing the error between the reference signal d(t), which closely matches or has some extent of correlation with the desired signal estimate and the beamformer output y(t) (equal to w.x(t)). This is a classical Weiner filtering problem for which the solution can be iteratively found using the LMS algorithm.

4.4.3 LMS algorithm formulation

From the method of steepest descent, the weight vector equation is given by [25],

$$x(n+1) = w(n) + \frac{1}{2}\mu\left[-\nabla\left(E\left\{e^2(n)\right\}\right)\right] \tag{4.11}$$

where μ is the step-size parameter and controls the convergence characteristics of the LMS algorithm; $e^2(n)$ is the mean square error between the beamformer output y(n) and the reference signal which is given by,

$$e^2(n) = \left[d^*(n) - w^h x(n)\right]^2 \tag{4.12}$$

The gradient vector in the above weight update equation can be computed as

$$\nabla_w\left(E\left\{e^2(n)\right\}\right) = -2r + 2Rw(n) \tag{4.13}$$

In the method of steepest descent the biggest problem is the computation involved in finding the values r and R matrices in real time. The LMS algorithm on the other hand simplifies this by using the instantaneous values of covariance matrices r and R instead of their actual values i.e.

$$R(n) = x(n)x^h(n) \tag{6.14}$$

$$r(n) = d^*(n)x(n) \tag{6.15}$$

Therefore the weight update can be given by the following equation,

$$\begin{aligned} w(n+1) &= w(n) + \mu x(n)[d^*(n) - x^h(n)w(n)] \\ &= w(n) + \mu x(n)e^*(n) \end{aligned} \tag{6.16}$$

The LMS algorithm is initiated with an arbitrary value w(0) for the weight vector at n=0. The successive corrections of the weight vector eventually leads to the minimum value of the mean squared error.

Therefore the LMS algorithm can be summarized in following equation

$$\begin{aligned} &Output, y(n) = w^h x(n) \\ &Error, e(n)d^*(n) - y(n) \\ &Weight, w(n+1) = w(n) + \mu x(n)e^*(n) \end{aligned} \tag{6.17}$$

(6.18)

4.4.4 Convergence and Stability of the LMS algorithm

The LMS algorithm initiated with some arbitrary value for the weight vector is seen to converge and stay stable for

$$0 \le \mu \le 1/\lambda_{\max} \tag{6.19}$$

where λ_{max} is the largest eigenvalue of the correlation matrix R. The convergence of the algorithm is inversely proportional to the eigenvalue spread of the correlation matrix R. When the eigenvalues of R are widespread, convergence may be slow. The eigenvalue spread of the correlation matrix is estimated by computing the ratio of the largest eigenvalue to the smallest eigenvalue of the matrix. If μ is chosen to be very small then the algorithm converges very slowly. A large value of μ may lead to a faster convergence but may be less stable around the minimum value.

4.5 RECURSIVE LEAST SQUARES ALGORITHM (RLS)

Contrary to the LMS algorithm, which uses the steepest descent method to determine the complex weight vector, the Recursive Least Squares (RLS) algorithm uses the method of least squares. The weight vector is updated by minimizing an exponentially weighted cost function consisting of two terms:

1.) sum of weighted error squares
2.) a regularization term.

Together the cost function is given by:

$$\varepsilon(k) = \sum_{i=1}^{k} \lambda^{k-i} \left| e(i)^2 \right| + \delta\lambda^k \left\| \overline{w}(k) \right\|^2 \tag{4.19}$$

where, *e(i)* is the error function defined by equation 4.1 and λ is called the *forgetting factor*, which is a positive constant close to, but less than one. It emphasizes past data in a non-stationary environment so that the statistical variations of the data can be tracked and not "forgotten". In a stationary environment, $\lambda = 1$ corresponds to infinite memory.

Expanding equation 4.26 and collecting terms, the weight summation of the covariance matrix for the received signal, $x(k)$, can be determined by:

$$\Phi(k) = \sum_{i=1}^{k} \lambda^{k-i} \bar{x}(k)\bar{x}^{H}(k) + \delta\lambda^{n} I \tag{4.20}$$

Performing the matrix inversion lemma to the result in equation 6.20, we can create a recursive equation to solve for the complex weight vector. A thorough description of the derivation is described in [19].

A summary of the RLS algorithm is provided below:

$$\bar{k}(k) = \frac{\lambda^{-1} P(k-1)\bar{x}(k)}{1 + \lambda^{-1}\bar{x}^{H}(k)P(k-1)\bar{x}(k)}$$

$$\begin{aligned} &e(k)d(k) - \bar{w}^{H}(k-1)\bar{x}(k) \\ &\bar{w}(k) = \bar{w}(k-1) + \bar{k}(k)e^{*}(k) \\ &P(k) = \lambda^{-1}P(k-1) - \lambda^{-1}\bar{k}(k)\bar{x}^{H}(k)P(k-1) \end{aligned} \tag{4.21}$$

At time sample $k = 1$, the initial conditions for the RLS algorithm can be described by:

1.) Set w(0) to either a column vector of all zeros, or to the first column vector of an *NxN* identity matrix.

2.) Setting $k = 0$ in equation 6.20 yields: $\Phi(0) = \delta I = P(0)$,

where,

$$\delta = \begin{cases} \text{small positive constant for high SNR} \\ \text{large positive constant for low SNR} \end{cases}$$

RLS is a desirable algorithm because it has the ability to retain information about the input data vector, $x(k)$, since the moment the algorithm was started. Therefore, the convergence of the RLS algorithm is much greater than that of the LMS algorithm by nearly an order of magnitude, but at the cost of increased computational complexity. An important feature of the RLS algorithm is its ability to replace the inversion of the covariance matrix in the Weiner solution with a simple scalar division.

4.6 Blind Adaptive Beamforming Algorithms [32],[33],[34],[35],[36],[37]

As was stated previously, "blind" adaptive algorithms do not need a training sequence in order to determine the required complex weight vector. They attempt to restore some type of property to the received signal for estimation. A common property in many digital modulation formats is the constant modulus of received signals. Therefore, this study focuses on blind adaptive algorithms which exploit this characteristic.

4.7 Constant Modulus Algorithm (CMA)

A typical digital signal possesses an envelope which is constant, on average. During transmission, corruption from the channel, multipath and noise can distort this envelope. Using the constant modulus algorithm (CMA), the envelope of the adaptive array output, *y(k)*, can be restored to a constant by measuring the variation in the signal's modulus and minimizing it by using the cost function defined below:

$$J(k) = E\left[\left|\left|y(k)\right|^{P} - 1\right|^{q}\right], p = 1,2; q = 1,2 \tag{4.22}$$

Taking the gradient of the above cost function yields:

$$\nabla(J(k)) = E\left[(|y(k)| - 1)\frac{\partial|y(k)|}{\partial \overline{w}^{*}(k)}\right]$$

$$= E\left[\left(|y(k)| - 1\right) \frac{\partial (y(k) y^*)(k))^{1/2}(k)}{\partial \bar{w}^*} \right]$$

$$= E\left[\left(|y(k)| - 1\right) \left(\frac{\partial (\bar{w}^H(k) \bar{x}(k) \bar{x}^H(k) \bar{w}(k))^{1/2}}{\partial \bar{w}^*(k)} \right) \right]$$

$$= \frac{1}{2} E\left[\left(|y(k)| - 1\right) \left(\bar{w}^H(k) \bar{x}(k) \bar{x}^H(k) \bar{w}(k) \right)^{-1/2} \frac{\partial (\bar{w}^H(k) \bar{x}^H(k) \bar{w}(k))}{\partial \bar{w}^*(k)} \right]$$

$$= \frac{1}{2} E\left[\left(|y(k)| - 1\right) \left(\frac{1}{y(k)} \bar{x}(k) \bar{x}^H(k) \bar{w}(k) \right) \right]$$

$$= \frac{1}{2} E\left[\left(1 - \frac{1}{|y(k)|} \right) \bar{x}(k) y^*(k) \right]$$

$$= \frac{1}{2} E\left[\bar{x}(k) \left(y(k) - \frac{y(k)}{|y(k)|} \right)^* \right] \qquad (4.23)$$

using the same equation for weight up-gradation as in LMS, and neglecting the expectation operator results in an iterative solution to solve for the complex weights using the instantaneous estimate of the gradient vector defined by:

$$\bar{w}(k+1) = \bar{w}(k) - \frac{1}{2} \mu \bar{x}(k) e^*(k) \qquad (4.24)$$

The constant modulus algorithm can be summarized as follows:

$$y(k) = \bar{w}^H(k) \bar{x}(k)$$
$$e(k) = y(k) - \frac{y(k)}{|y(k)|} \qquad (4.25)$$
$$\bar{w}(k+1) = \bar{w}(k) - \frac{1}{2} \mu \bar{x}(k) e^*(k)$$

where, w(0) is equal to the first column vector of an *NxN* identity matrix corresponding initially to an isotropic antenna array.

It is apparent from the error equation of CMA given above that there exist two conditions when error is equal to zero.

1.) When the output of the array is equal to unity magnitude.
2.) When the output of the array equals zero.

Second condition is not practical, since in order for the output of the array to be equal to zero when a signal is incident upon the antenna array, the weight vector must be equal to zero. This is a trivial and uninteresting solution. Additionally, it is possible for the constant modulus cost function to have false minima due to the fact that it is not convex in nature. If a weight vector produces an output with a constant envelope then so does its phase shifted version given by:

$$\overline{w}_r = e^{j\phi}\overline{w} \tag{4.26}$$

This can lead to phase ambiguity where the phase of the array output is undefined. The above solution for $p = 1$ & $q = 2$ is the typical form of the constant modulus algorithm. However, there do exist other forms for different p & q values which are summarized below:

$$\begin{aligned} p=1, q=1: &\qquad e(k) = \frac{y(k)}{|y(k)|}\operatorname{sgn}\left(|y(k)|-1\right) \\ p=2, q=1: &\qquad e(k) = 2y(k)\operatorname{sgn}\left(|y(k)|^2-1\right) \\ p=2, q=2: &\qquad e(k) = 4y(k)\operatorname{sgn}\left(|y(k)|^2-1\right) \end{aligned} \tag{4.27}$$

where, sgn( ) is the signum function defined by:

$$\operatorname{sgn}(x) = \begin{cases} -1, & x < 0 \\ 0, & x = 0 \\ 1, & x > 0 \end{cases} \tag{4.28}$$

CHAPTER 5: ADAPTIVE BEAMFORMING FOR OFDM SYSTEMS

In this chapter, we propose a novel frequency-domain beamforming algorithm for OFDM systems to suppress interference in a multipath environment. The type of interference that we are interested is hostile and the goal of interferers is to destroy the integrity of the signal transmitted by the desired user to the intended receiver. This type of interfering signal is referred to as a jamming signal. Although there are many research activities in OFDM, only a few numbers of them involve in adaptive beamforming for OFDM systems. Kim and Lee [40] proposed a time-domain beamforming strategy for an OFDM system in an AWGN channel with the presence of other users. On the other hand, Li and Sollenberger [21] proposed the MMSE diversity combiner using the parameter estimator to suppress co channel interference in a two-ray channel model. However, none of them considers the case of having interference power higher than the received power of the desired user. Moreover, none of them considers the performance of an adaptive antenna array for OFDM systems in the environment that is rich in multipaths, which is the main focus of this research.

5.1 Adaptive Beamforming Algorithm Used in Simulation

In this project, the adaptive beamforming algorithms that we use for simulation of adaptive beamforming in an OFDM system are the LMS algorithm, the RLS algorithm, and the CMA algorithm. As mentioned earlier, the frequency-domain beamforming processes the data on the subcarrier basis. Thus weights on each subcarrier should be updated across time, not frequency. We use the LMS algorithm as a reference here, as an example to explaining the implementation of our system for an OFDM modem.

5.2 Performance in Two-ray Channel

The number of subcarriers processed by each beamformer may increase depending on the frequency-selectivity of the channel. If the channel frequency response is relatively flat across several subcarriers, it is possible for each beamformer to process data across several subcarriers that have similar channel frequency response. However, as the channel frequency response across them starts to vary, the effectiveness of each beamformer to minimize the impact of the multiplicative distortion on data symbols across multiple subcarriers decreases.

As an illustration of the performance limitation of a single beamformer on the number of subcarriers under the frequency-selective environment, we consider a two-ray multipath channel. Figure 5.1 shows the channel impulse response of these two multipaths along with AWGN.

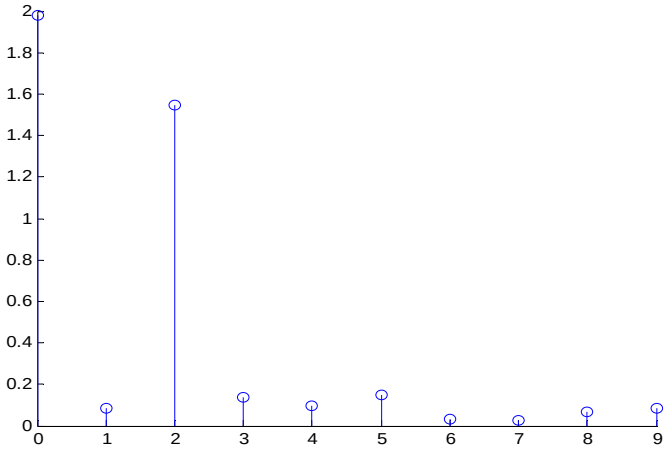

Figure 5.1: channel impulse response of two ray channel

We see that the channel impulse response gives us the delay spread of the channel.

Figure 5.2 shows the corresponding sampled channel frequency response observed by a 512-subcarrier OFDM system. We assume that the channel frequency response is flat from the each subcarrier perspective. Figure 5.2 shows both the magnitude plot (Fig: 5.2a) and the phase plot (Fig: 5.2b) for the channel frequency response. It is important to note that the frequency-selectivity of the channel increases as the delay spread increases [4].

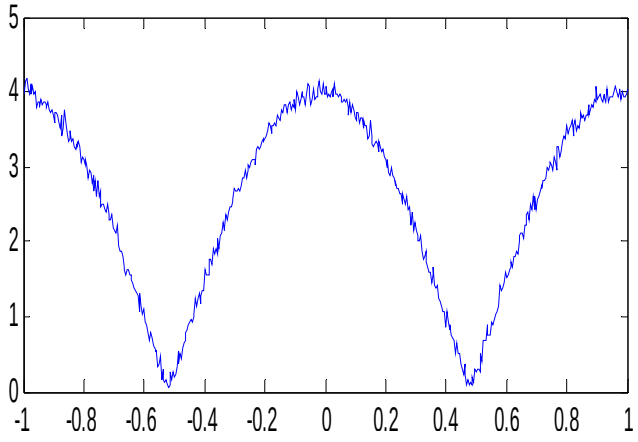

Figure 5.2(a): magnitude plot of channel frequency response

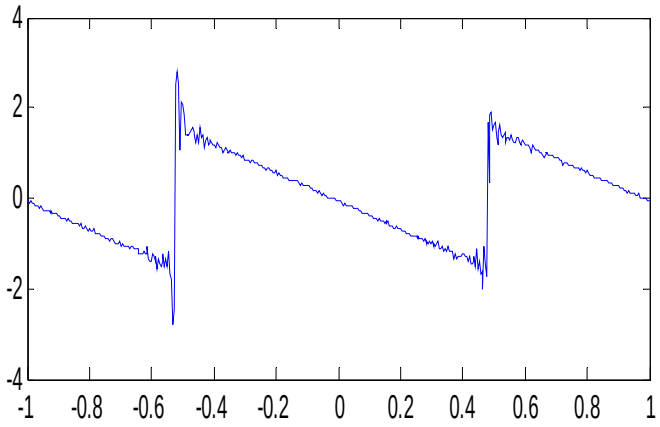

Figure 5.2(b): phase plot of channel frequency response

A signal constellation diagram is provided to give one the insight of effectiveness of using beamformers for suppressing the multiplicative distortion associated with demodulated symbols. Figure 5.3 shows the QPSK constellation diagram for a 512 carrier OFDM system, at the receiver end, before the application of beamforming algorithm.

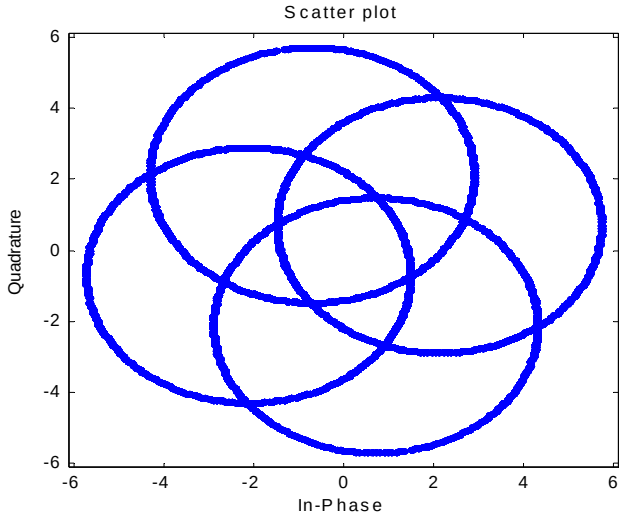

Figure 5.3: QPSK constellation diagram

Figure 7.5 shows the QPSK constellation diagram for the same system after application of the beamforming algorithm.

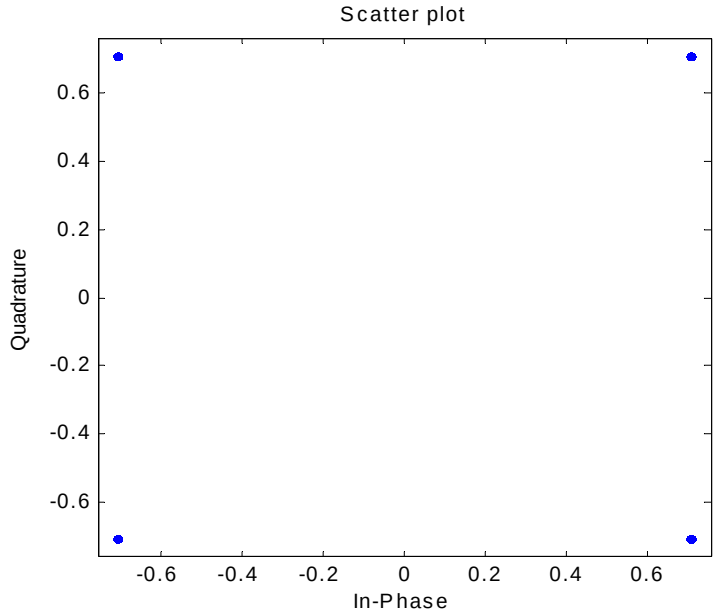

Figure 5.4: QPSK constellation diagram after convergence of the beamformer

From figure 5.4 we see that the beamformer effectively reduces the channel distortion and relieves us of the equalization and channel estimation stages completely. In both these cases, we assume that the guard time is greater than the delay spread to avoid ISI and AWGN is present. Furthermore, we insert pilot symbols across all the subcarriers and the LMS algorithm has converged before the decoding process begins. Using one frequency-domain beamformer per subcarrier, the multiplicative distortion associated with each demodulated symbols is largely suppressed for both channels. This shows that the performance of the frequency-domain beamforming is independent of the delay spread of the channel when each beamformer processes data symbols on one subcarrier only.

As a result, the number of beamformers required for this frequency-domain beamforming scheme depends on how frequency selective a channel is. For a given bandwidth of an OFDM signal, the bandwidth of each subcarrier decreases as the number of subcarriers increases and the channel frequency responses become very similar across several adjacent subcarriers. In this case, it is possible to apply a single beamformer for a number of symbols on the neighboring subcarriers to reduce computational complexity. In general, one needs to make the tradeoff between the computational complexity and the BER performance.

5.3 System Parameters

A bit stream generated by the source is modulated using shifted Quadrature Phase Shift Keying (QPSK). Then these bits are converted from serial-to-parallel and virtual carriers are added before subcarrier modulation, implemented through IFFT. Virtual carriers are zero padded to increase FFT resolution to prevent aliasing. Finally the baseband symbol is modulated using a high frequency carrier. The OFDM symbols are transmitted through a two ray channel with Additive White Gaussian Noise (AWGN). We define a transmitted frame which consists of 100 OFDM symbols. In order to facilitate the convergence of the LMS algorithm, we send the first 25 symbols as the training symbols, leaving 75 symbols as the data symbols in a frame. The training symbols are used as the desired symbols to facilitate the convergence of the algorithm at the beginning of the frame. The algorithm then switches to the decision-directed mode during the data portion of the frame to update the weight vector for tracking the time-varying nature of the channel. During the decision-directed mode, the desired signal is the symbol at the output of the decision device. We set the convergence rate of LMS algorithm at 0.006. We implement an OFDM system with 512 sub-carriers, out of which 416 (81.25%) are active carriers, carrying data and the other 96 are virtual carriers.

We assume the receiver is equipped with a five element ULA with half wavelength spacing between the elements. Each element of the antenna array is assumed to be isotropic. Figure 5.5 shows the simulation block diagram used for the evaluation of our proposed beamforming algorithm.

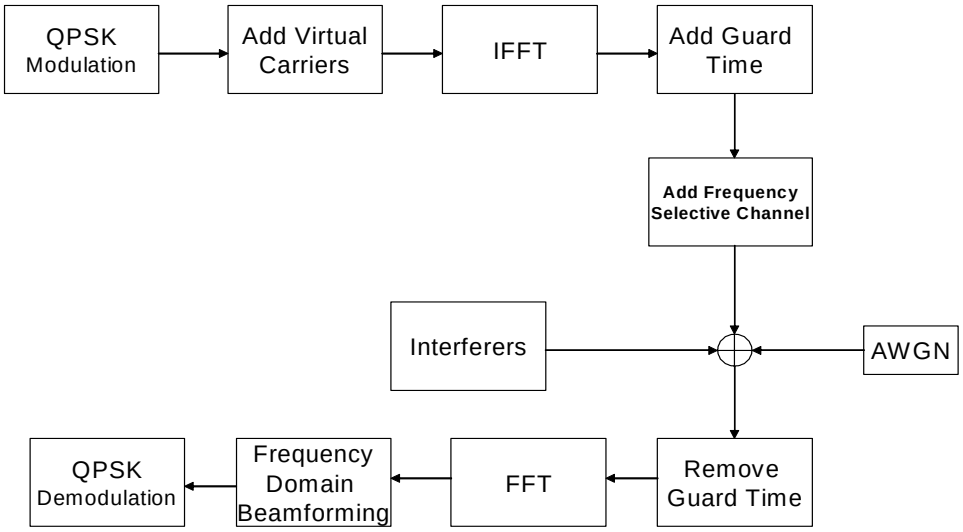

Figure 5.5: Simulation block diagram for an OFDM system using frequency-domain beamforming.

The performance of the algorithm has also been analyzed by changing various system parameters. A plot of bit error rates for different values of μ is shown in Figure 5.6

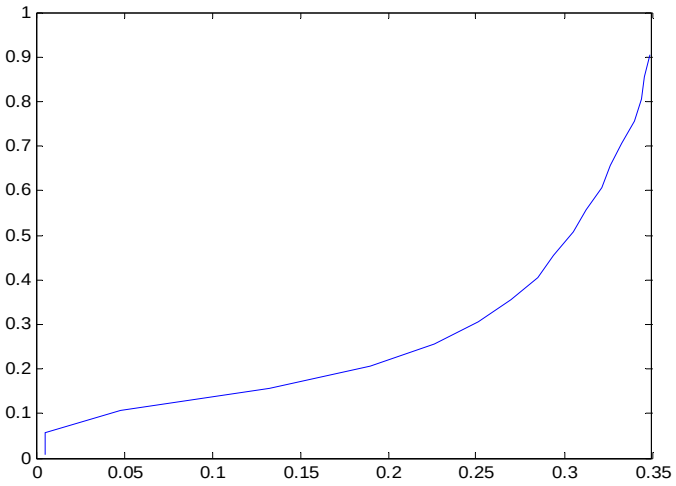

Figure 5.6: Plot of BER vs. different values of μ

We see that the performance of LMS algorithm degrades with increase in the step size. This can be contributed to the fact that with increase in the step size the algorithm performs analysis of given data in lesser detail. Thus, a drop in accuracy. However, this increase in step size does increase the speed of convergence.

A plot of bit error rate and the number of symbols is given in Figure 5.7. The performance of algorithm improves as the number of symbols is increased.

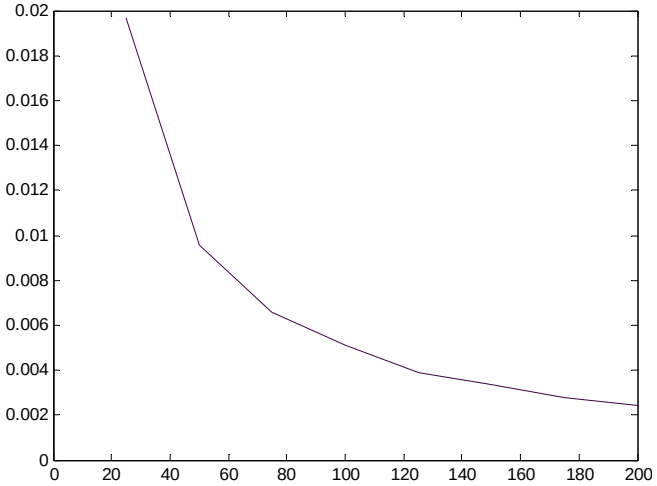

Figure 5.7: plot bit error rate vs. number of symbols

Figure 5.8 shows a plot of BER vs SNR for an AWGN channel. It shows that the BER drops with increase in the SNR. That is, as the signal power is raised in reference to the channel noise, the BER of the system decreases.

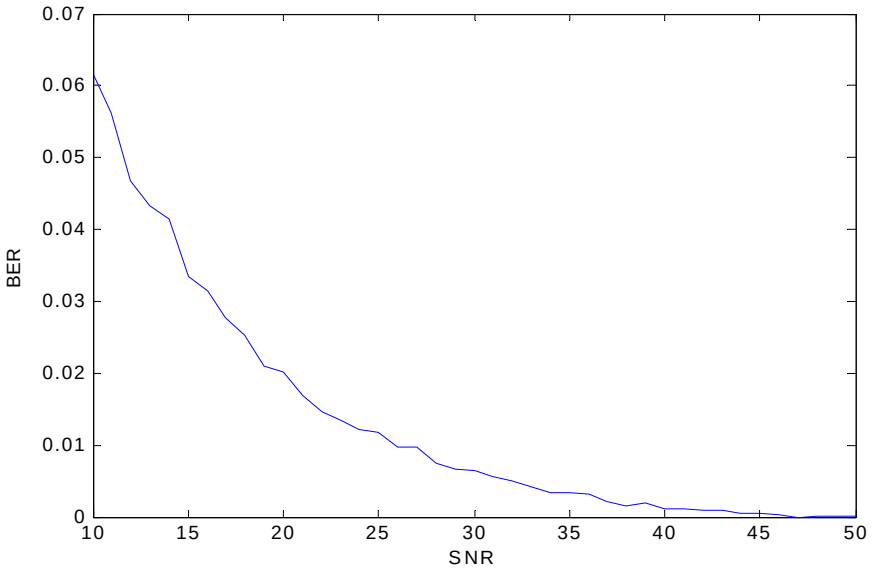

Figure 5.8: Plot of BER vs SNR

CHAPTER 6: SIMULATION RESULTS

In this chapter, we present the results of the simulations of proposed algorithms for beamforming in OFDM systems, in the presence of interference.

6.1 LMS

To observe the interference suppression capability for the frequency-domain beamforming scheme, we will observe the beam pattern for LMS beamformers under the interference environment; first with just AWGN and then for a channel which consists of AWGN plus two wideband jammers with jamming power higher than the received power of the desired signal.

Figure 6.1 below shows a plot of mean square error against the number of iterations, which effectively shows the convergence characteristics of LMS algorithm; this plot is generated for five hundred symbols and four hundred and sixteen active subcarriers. These simulations are run under the conditions encountered in a channel with AWGN. The convergence plot shows that LMS algorithm follows a slow convergence rate. Here we see that the mean square error does not completely converge until the seventieth iteration, which is noticeably slower than other algorithms. Thus, the attraction of LMS does not lie in its convergence capabilities, but in its computational simplicity.

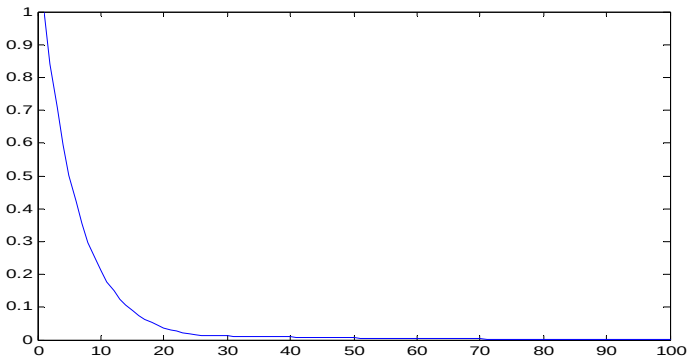

Figure 6.1: plot of mean square error vs. number of iterations

Figure 6.2 shows the polar beam pattern of the uniform linear array for 5 element array, with the user at 60^{o}. The simulation shows that the main lobe of the beam is being

directed fully in the direction of the desired user. This shows successful performance of adaptive beamforming by LMS algorithm.

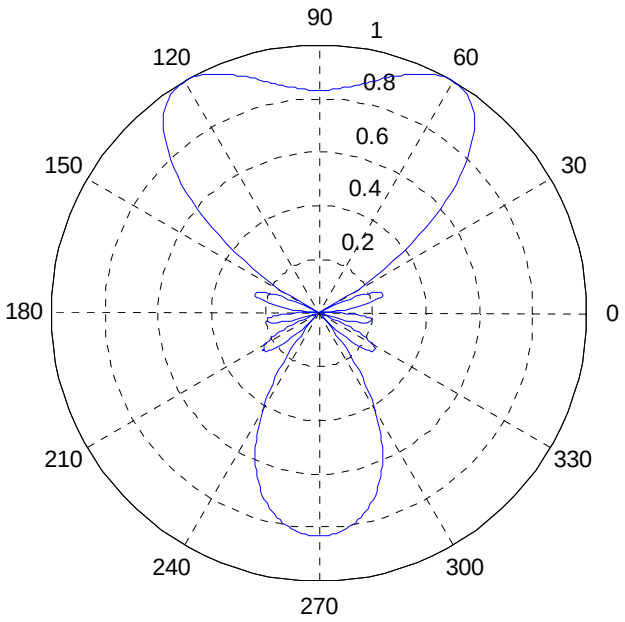

Figure 6.2: Polar Beam Pattern for LMS, with user at 60^{o}

Figure 6.3 shows the amplitude response pattern of the antenna array. It shows a plot of the amplitude of the antenna gain, against the angle of arrival (AOA) of the received signal.

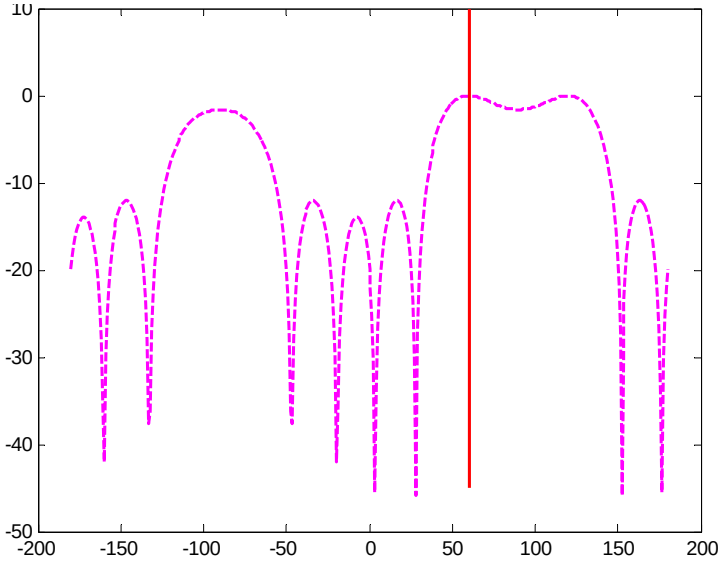

Figure 6.3: amplitude response pattern of LMS with user at 60^{o}

The red line depicts the AOA of the desired user. Note that the antenna array adapts its radiation pattern to provide maximum gain at the AOA of desired signal.

6.2 LMS with Jammers

Now, we analyze the performance of our algorithm for a case with two jammers present. The desired user is located at 30^{o} and the jammers are at -25^{o} and -125^{o} respectively, with respect to the array normal. A five element uniform linear array (ULA) is assumed to be deployed at the receiver side. Figure 6.4 shows the beam patterns of the beamformers for a 512-subcarrier OFDM system under the AWGN channel. It shows that the beamformers steer the beam towards the direction of the desired user and at the same time place null towards the direction of the jammers. The desired signals at all subcarriers have a positive gain over all the jamming signals. This shows that our frequency-domain beamforming scheme is very effective for suppressing the jamming signals which have higher power than the desired signal.

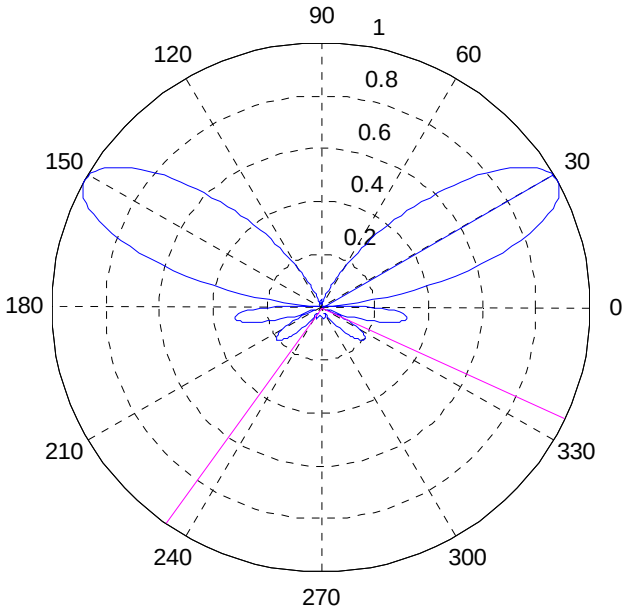

Figure 6.4: Polar Beam Pattern for LMS, with user at 30^{o}; jammers at -25^{o} and -125^{o}

Figure 6.5 shows the amplitude response pattern of the antenna array. The red line depicts the AOA of the desired user, while the blue lines are the AOA of jamming signals. Note that the antenna array adapts its radiation pattern to provide maximum gain at the AOA

of desired signal, while at the same time the gain of antenna arrays is minimized in the direction of the jamming signals.

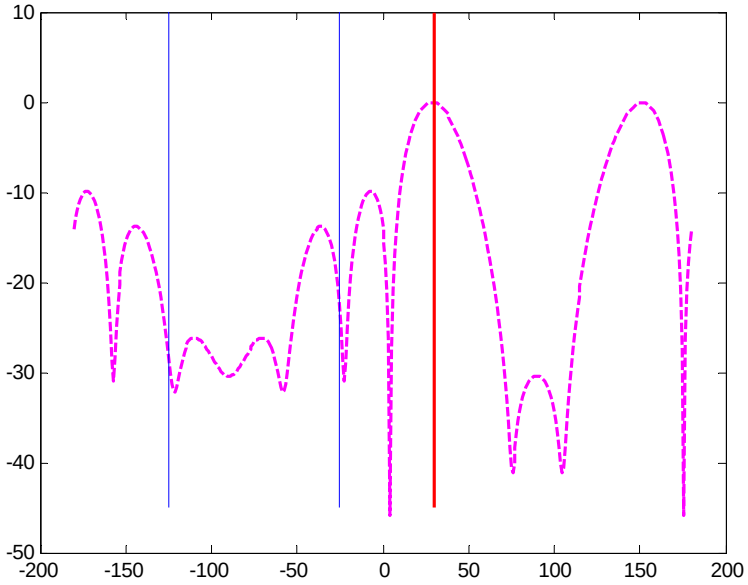

Figure 6.5: amplitude response pattern of LMS: user at 30^{o}; jammers at -25^{o} and -125^{o}

6.3 LMS for Multi-Users

The performance of LMS algorithm has also been analyzed for multiple users, at different spatial locations. Figure 6.6 shows the convergence plots for two users in a multi-user scenario. Figure 6.6(a) shows convergence of MSE for user 1 while figure 6.6(b) shows convergence for user 2. It can be seen that convergence of MSE for both users is similar.

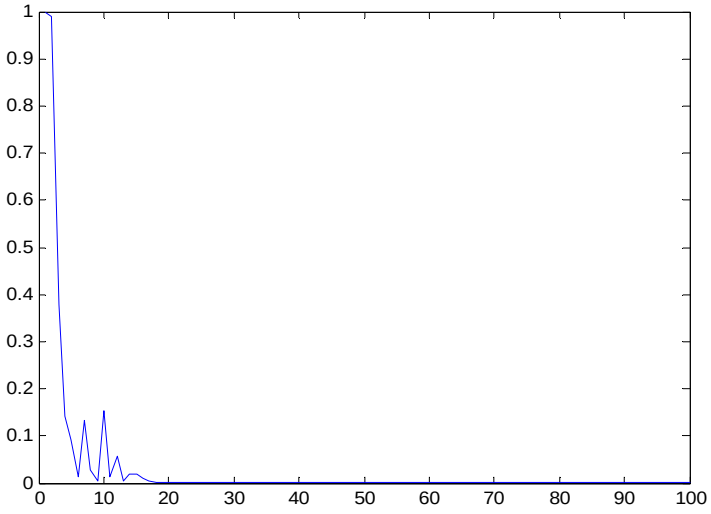

Figure 6.6 (a): Convergence plot of user 1 for multi-user LMS

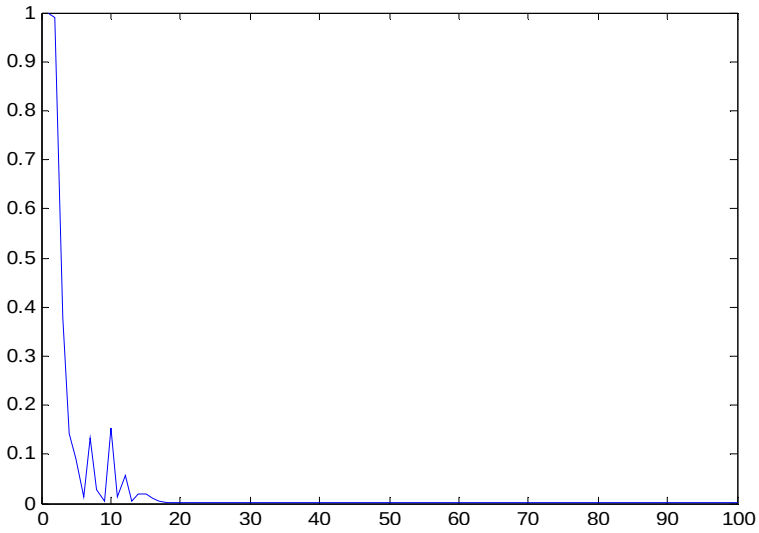

Figure 6.6(b): Convergence plot of user 2 for multi-user LMS

Figure 6.7 shows the beampattern for both the users. The first user is at 60^{o} and the second user is at 145^{o}. The figure below shows that the main lobe of the beam is being directed fully in the direction of the desired user in both cases. This shows successful performance of adaptive beamforming by LMS algorithm in a multi-user scenario.

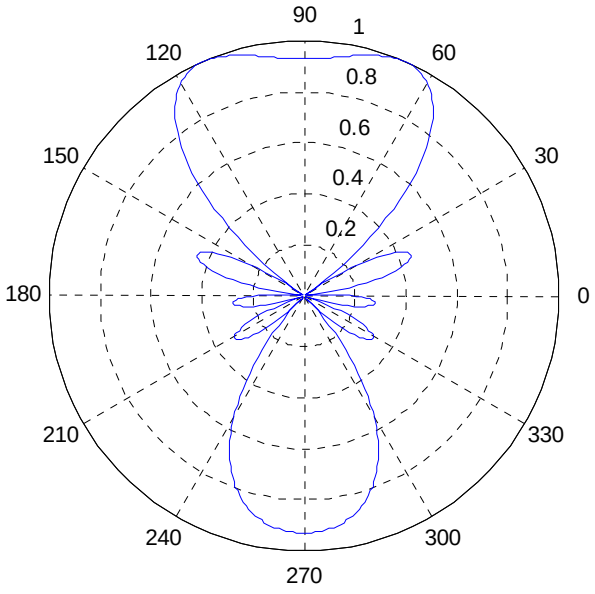

Figure 6.7(a): Polar Beam Pattern of user 1at 60^{o}, for LMS, with multi-users

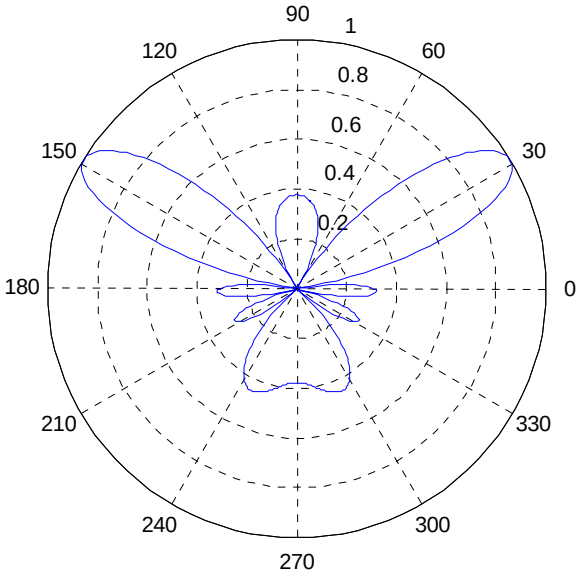

Figure 6.7(b): Polar Beam Pattern of user 2at 145^{o}, for LMS, with multi-users

6.4 RLS

Figure 6.8 below shows a plot of mean square error against the number of iterations, which effectively shows the convergence characteristics of RLS algorithm; this plot is generated for five hundred symbols and four hundred and sixteen active subcarriers. These simulations are run under the conditions encountered in a channel with additive white Gaussian noise (AWGN). The figure depicts the fast convergence property of RLS algorithm. We can notice from the plot that mean square error for RLS algorithm converges completely well before the tenth iteration, which is much faster than the LMS algorithm convergence rate. However, this is achieved at the price of computational complexity.

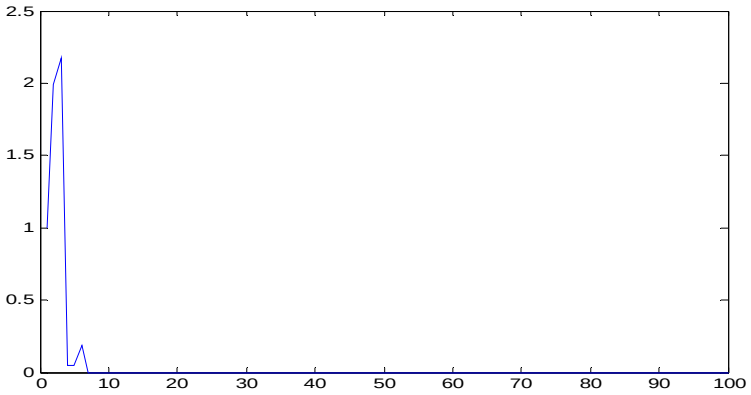

Figure 6.8: BER Convergence plot for RLS Algorithm

Figure 6.9 shows the polar beam pattern of the uniform linear array for 5 element array, with the user at 90^{o}. The simulation shows that the main lobe of the beam is being directed fully in the direction of the desired user. This shows successful performance of adaptive beamforming by RLS algorithm.

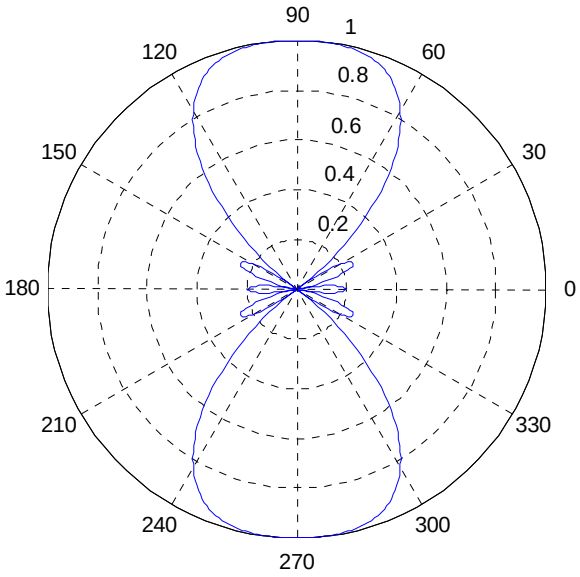

Figure 6.9: Polar Beam Pattern for RLS, with user at 90^{o}

Figure 6.10 shows the amplitude response pattern of the antenna array. It shows a plot of the amplitude of the antenna gain, against the angle of arrival (AOA) of the received signal. The successful beamforming by RLS algorithm is shown, as the antenna array provides maximum antenna gain in the desired direction, depicted by the red line.

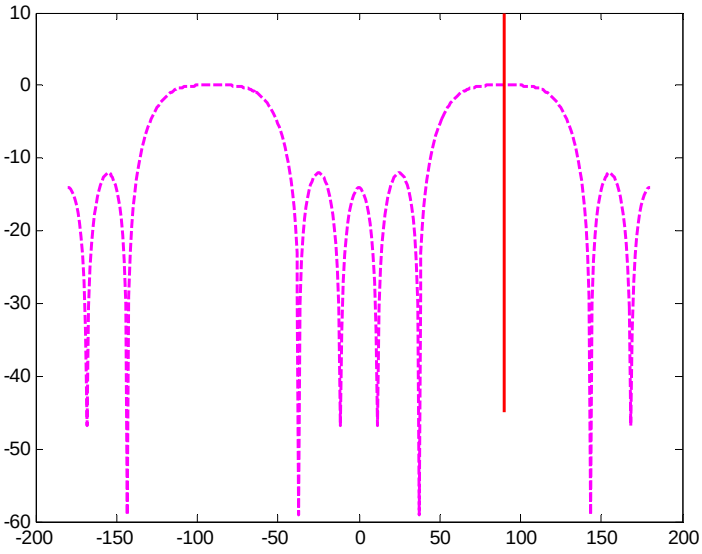

Figure 6.10: amplitude response pattern of RLS with user at 90^{o}

6.5 RLS with Jammers

Now, we analyze the performance of our algorithm for a case with two jammers present at 30^o and 150^o respectively. In addition the channel also undergoes AWGN. Figure 6.11 shows the polar beam pattern of the 5 element array, with the user at 0^o. The jamming signals are depicted by the two red lines at their respective spatial location. The simulation shows that the main lobe of the beam is being directed fully in the direction of the desired user. At the same time we can note that nulls are being placed in the direction of the jamming signals, thus, interference from jammers is being effectively suppressed. This shows successful performance of adaptive beamforming by RLS algorithm, in the presence of jammers.

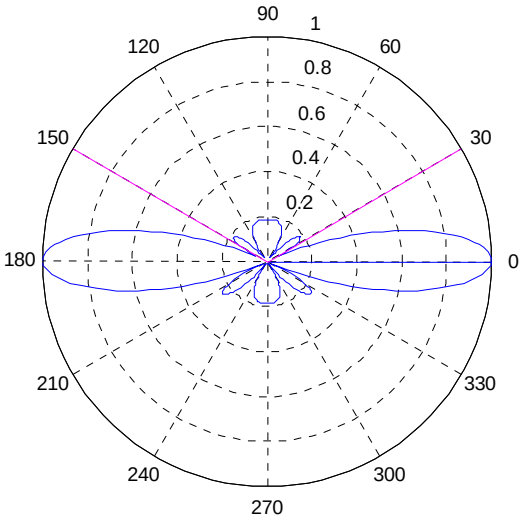

Figure 6.11: Polar Beam Pattern for RLS, with user at 90^o; jammers at 30^o and 150^o

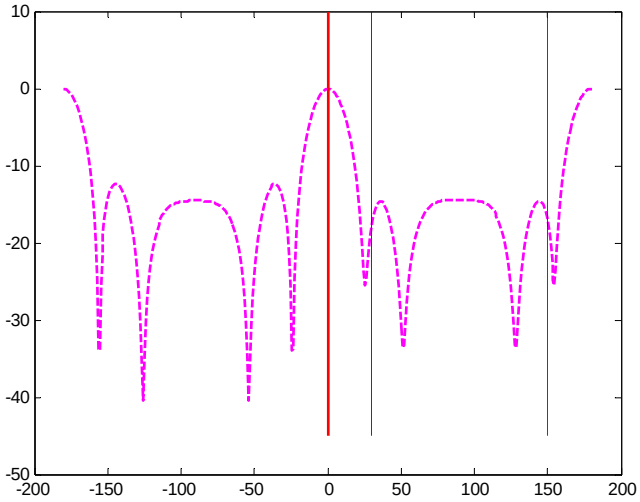

Figure 6.12: amplitude response pattern of RLS with user at 90^o; jammers at 30^o and 150^o

The figure above shows the amplitude response pattern of the antenna array. The red line depicts the AOA of the desired user. The blue lines show the AOA of the interfering (jamming) signals. Note that the antenna array adapts its radiation pattern to provide maximum gain at the AOA of desired signal, while at the same time the gain of antenna arrays is minimized in the direction of the jamming signals.

6.6 RLS for Multi-Users

RLS algorithm has also been run for multiple users and its performance analyzed, with users at different spatial locations. Figure 6.13 shows the convergence plots for two users in a multi-user scenario.

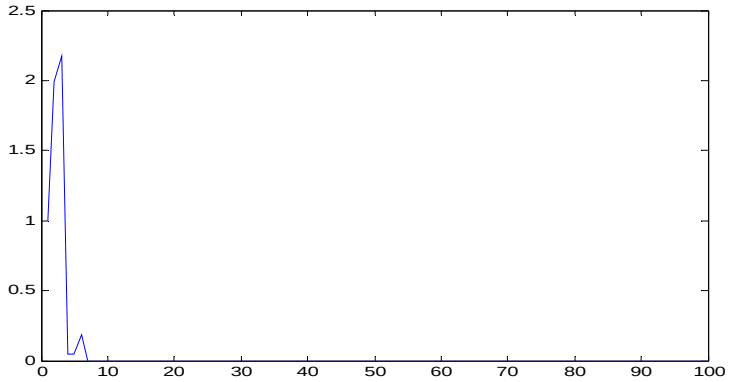

Figure 6.13(a): plot of mean square error vs. number of iterations for user 1

Figure 6.13(a) shows convergence of MSE for user 1 while figure 6.13(b) shows convergence for user 2. The convergence rate for both the users is similar.

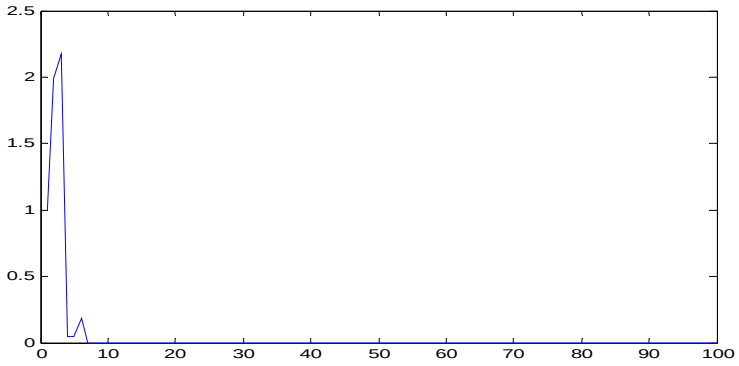

Figure 6.13(b): plot of mean square error vs. number of iterations for user 2

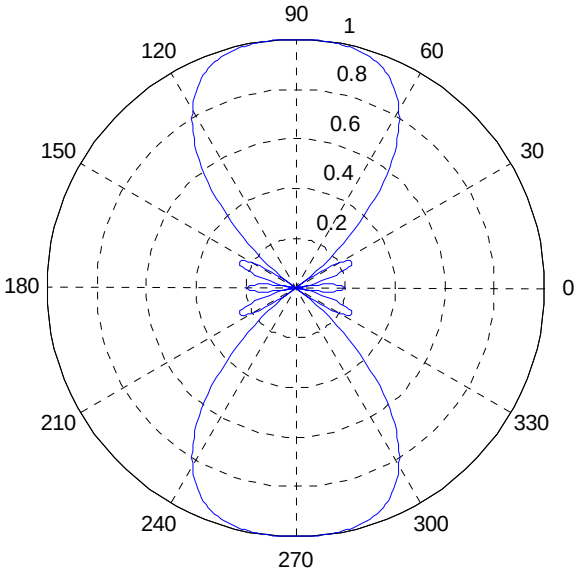

Figure 6.14(a): Polar Beam Pattern of user 1at 90^{o}, for RLS with multi-users

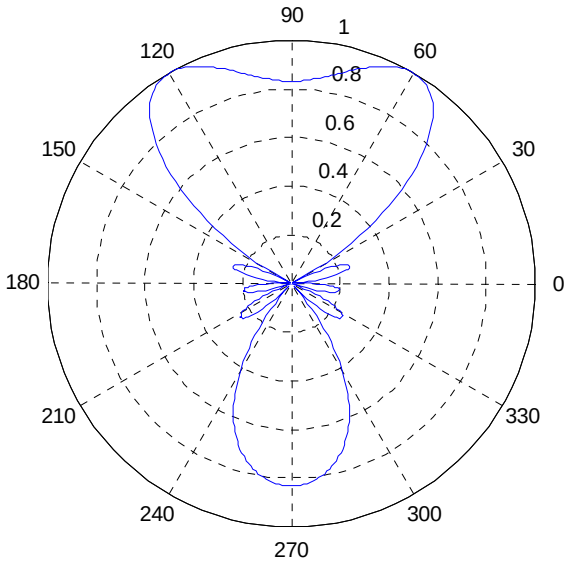

Figure 6.14(b): Polar Beam Pattern of user 2 at 60^{o}, for RLS with multi-users

Figure 6.14(a) shows the beampattern for user 1 and figure 6.14(b) for user 2. The first user is at 90^{o} and the second user is at 60^{o}. The figures above shows that the main lobe of the beam is being directed fully in the direction of the desired user in both cases. This shows successful performance of adaptive beamforming by LMS algorithm in a multi-user scenario.

6.7 CMA

Figure 6.15 below shows a plot of mean square error against the number of iterations, which effectively shows the convergence characteristics of CMA algorithm; this plot is generated for five hundred symbols and four hundred and sixteen active subcarriers. These simulations are run under the conditions encountered in a channel with additive white Gaussian noise (AWGN).

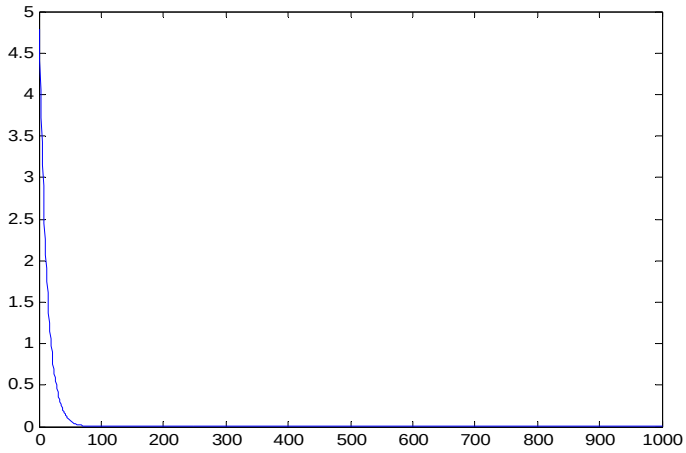

Figure 6.15: plot of mean square error vs. number of iterations

This plot depicts the convergence rate of CMA which is slower than RLS but still faster than LMS. However, the main benefit of CMA is in its being able to work without any reference signal.

Figure 6.16 shows the polar beam pattern of the uniform linear array for 5 element array, with the user at 30^{o}. The simulation shows that the main lobe of the beam is being directed fully in the direction of the desired user. This shows successful performance of adaptive beamforming by CMA algorithm.

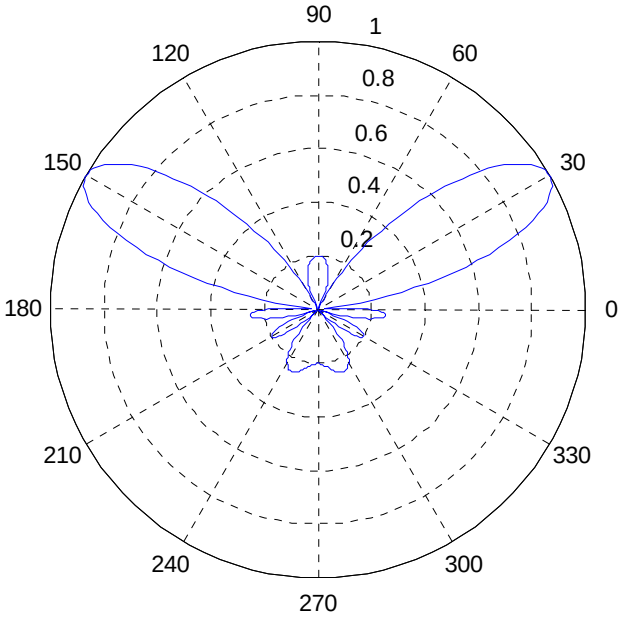

Figure 6.16: Polar Beam Pattern for CMA, with user at 30^{o}

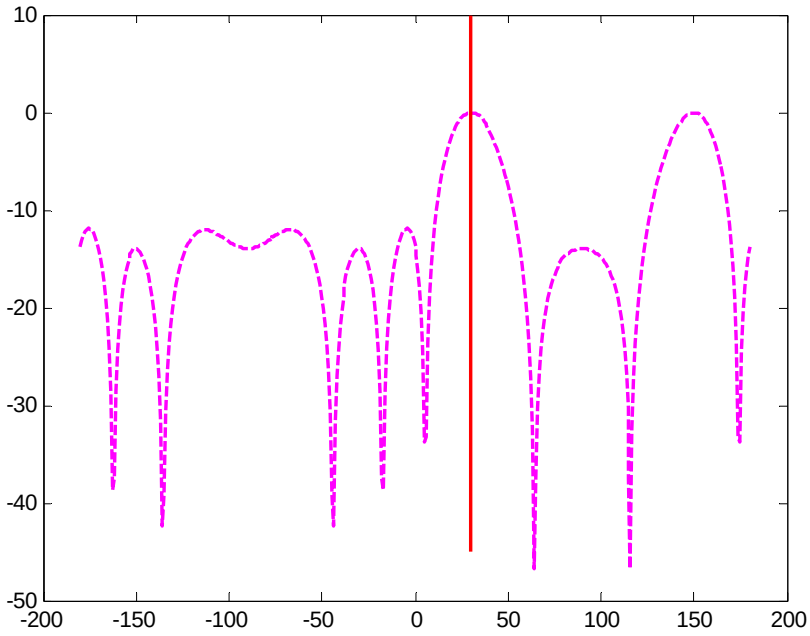

Figure 6.17: amplitude response pattern of CMA with user at 30^{o}

Figure 6.17 shows the amplitude response pattern of the antenna array. It shows a plot of the amplitude of the antenna gain, against the angle of arrival (AOA) of the received signal. The red line depicts the AOA of the desired user. Note that the antenna array adapts its radiation pattern to provide maximum gain at the AOA of desired signal.

CHAPTER 7: DSK TMS320C6713 IMPLEMENTATION

7.1 INTRODUCTION

The 6713 DSP Starter Kit (DSK) is stand alone evaluation platform for the TMS320C6713 Digital Signal Processor. It includes a target board that can be used as a reference design for interfacing the DSP to common devices such as SDRAM, Flash, etc. An on-board JTAG emulator allows debug from Code Composer Studio through the PC's USB port. For details on installation and usage, please consult the User's Manual provided with the project documentation.

7.2 Components

- A TMS320C6713 Digital Signal Processor has an operating frequency of 225 MHz.
- It has 16MB DRAM.
- 512 Kb of non-volatile Flash Memory
- Standard Expansion connectors
- Single voltage power supply (+5V)

7.3 Working

The DSP interfaces to on-board peripherals through a 32-bit wide EMIF(External Memory Interface. The SDRAM, Flash and CPLD registers are all connected to the bus.
Code composer communicates with the DSK with the DSK through an embedded JTAG emulator with a USB host interface.
When the DSK is powered up the embedded USB controller will boot up and wait for enumeration from the host. Once the host has enumerated, Code Composer can be started. When Code Composer is started the emulation driver will make contact with the DSK. It will then download the emulation firmware to the DSK. Once that is complete the firmware will disconnect from the USB bus and reconnect as an emulator.

7.3.1 Limitations

One limitation is that only one DSK per PC is supported.

7.4 ARCHITECTURE

7.4.1 Memory Map

It has a large byte addressable address space. Program code and data can be placed anywhere in the address space. Addresses are 32-bits wide.

Table 7.1 shows the memory map of the address space of a generic C6713 processor. The internal memory sits at the beginning of the address space. Portions of internal memory can be reconfigured in software.

Address	C6713 Memory Type
0x00000000	Internal memory
0x00030000	Reserved or peripheral
0x80000000	SDRAM
0x90000000	Flash CPLD 0x90080000
0xA0000000	Daughter Card
0xB0000000	

Table 7.1: Memory map of address space for C6713

7.4.2 Board Components

- CPLD
- MISC Register
- Synchronous DRAM
- Flash Memory
- Daughter Card Interface

CPLD Programmable Logic:

It is used to implement:

1. 4 x memory-mapped control/status registers that allow software control
2. Control of daughter card interface and signals
3. assorted glue logic that ties the board components together

MISC Register:

It is used to provide software control for miscellaneous board functions. It controls how auxiliary signals are brought out to the daughter-card connectors.

Synchronous DRAM:

The DSK uses a 128 Mb SDRAM on the 32-bit EMIF. It is mapped at 0x80000000. total available memory is 16 MB.

Flash Memory:

Flash is a type of memory which does not lose its contents when the power is turned off. When read, it looks like a simple synchronous ROM. It can be erased in large blocks referred to as pages or sectors.

The DSK uses a 512 KB external flash as a boot option

Daughter Card Interface:

The DSK provides three expansion connectors that can be used to accept plug-in daughter cards. The daughter card allows users to build their DSK platform to extend the capabilities and provide customer and application specific I/O. the expansion connectors are for memory, peripherals and Host Port Interface (HPI).

7.4.3 Board Layout

C6713 is 8.75x4.5 inch multilayer board powered by an external +5V only supply. Figure7.2 shows its layout.

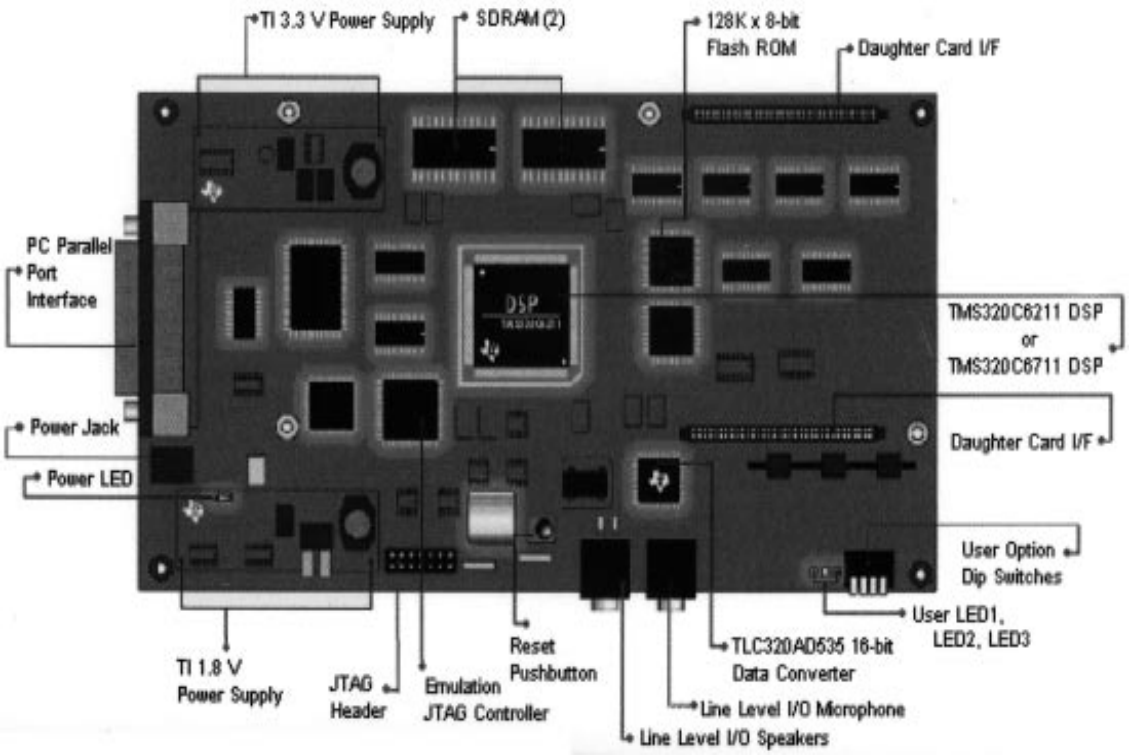

Figure 7.2 Layout of C6713

7.4.4 Connector Index

Connector	# of Pin	function
J4	80	Memory
J3	80	Peripheral
J1	80	HPI
J301	3	Microphone
J303	3	Line in
J304	3	Line out
J303	3	Headphone
J5	2	+5V
J8	14	External JTAG
J201	5	USB port
JP3	10	CPLD programming

Table 7.2 Connector index of C6713

CHAPTER 8 : CONCLUSIONS AND FUTURE WORK

8.1 Conclusions

In this thesis, we study the adaptive array algorithms for OFDM systems. The nature of the multicarrier communication gives new challenges for applying adaptive beamforming to OFDM. We propose a frequency-domain beamforming scheme for conventional OFDM systems which operate under a frequency-selective environment. The main idea behind this scheme is to employ multiple beamformers, with each beamformer combining symbols for each subcarrier. Using the MMSE criterion, this scheme can minimize the effect of multipath distortion introduced by the frequency-selective channel without the loss of the AOA information. The proposed beamforming algorithm has been studied in both flat fading and frequency-selective fading channels with the presence of interference. Simulation results show that using individual beamformers to process data symbols on each subcarrier has a better performance than using one beamformer only under the narrowband jammer case in the flat fading channel. We also show that under the frequency selective fading channel model, the total number of beamformers can be fewer than the number of subcarriers for OFDM systems with 512 subcarriers without significant performance degradation. At the beginning of this thesis, we also introduce a basis concept of OFDM and the fundamentals of adaptive antenna array.

8.2 Future Work

The following lists some of the possible of future work on adaptive beamforming for OFDM systems.

1) In this thesis, we only evaluate the performance of the beamforming algorithms for the receiver employing ULA. It may be useful to study its performance for different array geometries, such as the circular array and the planar array.

2) In this research, we only employ a single algorithm for the frequency-domain beamforming scheme. After the RLS algorithm converges, it may be possible to use the LMS or the normalized LMS algorithm to reduce the computational complexity. Also,

the performance of the adaptive beamforming algorithm using the LMS algorithm in the decision-directed mode should be examined in the future.

3) In this project, we assume no carrier frequency offset between the transmitter and receiver and also perfect symbol timing at the receiver. In the future, we can examine the performance of the beamforming algorithms under the frequency offset, phase noise, and symbol timing error conditions.

4) Last but not least, it will be useful to implement the proposed beamforming algorithms on a FPGA board and construct the multiple element antenna array for field trial testing.

REFERENCES

[1] J. M. Pereira, "Balancing Public and Private in Fourth Generation," *The 12th IEEE International Symposium on Personal, Indoor and Mobile Radio Communications*, vol. 2, pp 125-132, Sept/Oct 2001.

[2] R. Van Nee and R. Prasad, *OFDM for Wireless Multimedia Communications*, Artech House Publishers, Massachusetts, 2000.

[3] B. Van Veen and K. Buckley, "Beamforming: A Versatile Approach to Spatial Filtering," *IEEE ASSP Magazine*, pp. 4-22, April 1988.

[4] Bing-Leung Patrick Cheung, "Simulation of Adaptive Array Algorithms for OFDM and Adaptive Vector OFDM Systems," *MS Thesis,* Virginia Polytechnic Institute and State University, Sept 2002.

[5] M. Russell and G. Stuber, "Interchannel Interference Analysis of OFDM in a Mobile Environment," *Proceedings of IEEE VTC'95*, Chicago, IL, July 1995, pp.820-824.

[6] P. Robertson and S. Kaiser, "The Effects of Doppler Spreads in OFDM(A) Mobile Radio Systems," *Proceedings of IEEE VTC'99-Fall,* 1999, pp. 329-333.

[7] Ahmad R. S. Bahai, Burton R. Saltzberg, "Multi-Carrier Digital Communications Theory and Applications of OFDM", *Kluwer Academic/Plenum Publishers.*

[8] C.A. Balanis, *Antenna Theory: Analysis and Desig*n, John Wiley and Sons, New York, 1997.

[9] J. Litva and T. Lo, "Digital Beamforming in Wireless Communications," *Artech House Publishers, Massachusetts, 1996.*

[10] S. Haykin, *Advances in Spectrum Analysis and Array Processing, Vol III*, Prentice Hall, New Jersey, 1991.

[11] B. Van Veen and K. Buckley, "Beamforming: A Versatile Approach to Spatial Filtering," *IEEE ASSP Magazine*, pp. 4-22, April 1988.

[12] A. V. Oppenheim and R. W. Schafer, *Discrete -Time Signal Processing*, Prentice Hall, New Jersey, 1989.

[13] Barry D. Van Veen and Kevin M. Buckley. Beamforming: A Versatile Approach to Spatial Filtering, IEEE ASSP Magazine, April 1998.

[14] – Lotter, Michiel; Van Rooyen, Pieter & Van Wyk, Danie. *Space – Time Processing For CDMA Mobile Communications.* Kluwer Academic Publishers. Boston-London.2000.

[15] Okamoto, Garret T. Smart Antenna Systems and Wireless Lans, New York Kluwer Academic Publishers, 2002.

[16] John Litva and Titus Kwok-Yeung Lo. Digital Beamforming in Wireless Communications, Artech House, Boston, 1996.

[17] Lal, C. Godara. Applications of Antenna Arrays to mobile Communications, Part I: Performance Improvement, feasibility, and System Considerations. Proceedings of the IEEE, Vol. 85, No. 7, July 1997.

[18] J. S. Blogh and L. Hanzo. Third Generation Systems and Intelligent Wireless Networking: Smart Antennas and Adaptive Modulation. John Wiley & Sons Inc. New York, 2002.

[19] N G Chee, Desmond. Smart Antennas for Wireless Applications and Switched Beamforming, undergraduate thesis, University of Queensland, School of Information Technology and Electrical Engineering, 2001.

[20] Kiran K. Shetty, "A Novel Algorithm for Uplink Interference Suppression Using Smart Antennas in Mobile Communications," MS Thesis, FAMU-FSU College of Engineering, Florida State University, 2004.

[21] Y. Li, N. R. Sollenberger, "Adaptive Antenna Arrays for OFDM Systems with Cochannel Interference," *IEEE Transactions on Communications*, vol. 47, no. 2, February 1999.

[22] P. Hoeher, S. Kaiser, and P. Robertson, "Two-dimensional Pilot-symbol-aided Channel Estimation by Wiener Filtering," *IEEE International Conference on Acoustics, Speech, and Signal Processing*, vol. 3, pp. 1845-1848, 1997.

[23] A. F. Eric OH. Smart Antennas and Dynamic Sector Synthesis, undergraduate thesis, University of Queensland, School of Information Technology and Electrical Engineering, 2001.

[24] Jack H. Winters. Smart Antennas for Wireless Systems, IEEE Personal Communications, February 1998

[25] Haykin, Simon. Introduction to Adaptive Filters. Macmillan Publishing Company, New York, 1985

[26] Lal, C. Godara. Applications of Antenna Arrays to mobile Communications, Part II: Beam-Forming and Direction-of-Arrival Consideration, Proceedings of the IEEE, Vol. 85, No. 8, August 1997.

[27] Kohei Mori, Study of Smart Antennas for High Speed Wireless Communications, Doctoral Disseration, Electrical and Computer Engineering, Yokohama National University, 2001

[28] J. Litva and T. Lo, *Digital Beamforming in Wireless Communications*, Artech House Publishers, Massachusetts, 1996.

[29] S. Haykin, *Adaptive Filter Theory,* 3rd edition, Prentice Hall, New Jersey, 1996.

[30] B. Farhang Boroujeny, "Adaptive Filters, Theory and Application," John Wiley, Chichester, West Sussex, July 2003.

[31] B. Van Veen and K. Buckley, "Beamforming: A Versatile Approach to Spatial Filtering," *IEEE ASSP Magazine*, pp. 4-22, April 1988.

[32] Compton, R.T. Jr. **"**Adaptive Antennas – Concepts and Performance," Prentice Hall, Englewood Cliffs, New Jersey. 1988.

[33] – Haykin, Simon. *Adaptive Filter Theory.* Prentice Hall, Englewood Cliffs, New Jersey. 3rd Ed. 1996.

[34] – Litva, John & Titus Kwok-Yeung Lo. *Digital Beamforming in Wireless Communications*. Artech House Publishers. Boston-London. 1996

[35] W. G. Jeon, K. H. Chang, and Y. S. Cho, "An Equalization Technique for Orthogonal Frequency-Division Multiplexing Systems in Time-Variant Multipath Channels," *IEEE Transactions on Communications*, vol. 47, No. 1, pp. 29-32, January 1999.

[36] – Proakis, John G. *Digital Communications.* 3rd Ed. McGraw Hill, New York, NY, 1995.

[37] – Shetty, Kiran K. "A Novel Algorithm for Uplink Interference Suppression Using Smart Antennas in Mobile Communications". *Master's Thesis, The Florida State University.* 2004.

[38] B. Widrow and M.E. Hoff. Adaptive Switch Circuits, IRE WESCOM, Conv. Rec., Part 4, 1960

[39] Jeffery D. Connor, " A Study of Despread-Respread Multi-Target Adaptive Algorithms in an AWGN Channel ", *Master's Thesis, The Florida State University. 2005*.